Published OnlineFirst May 18, 2010; DOI:10.1158/0008-5472.CAN-09-4210

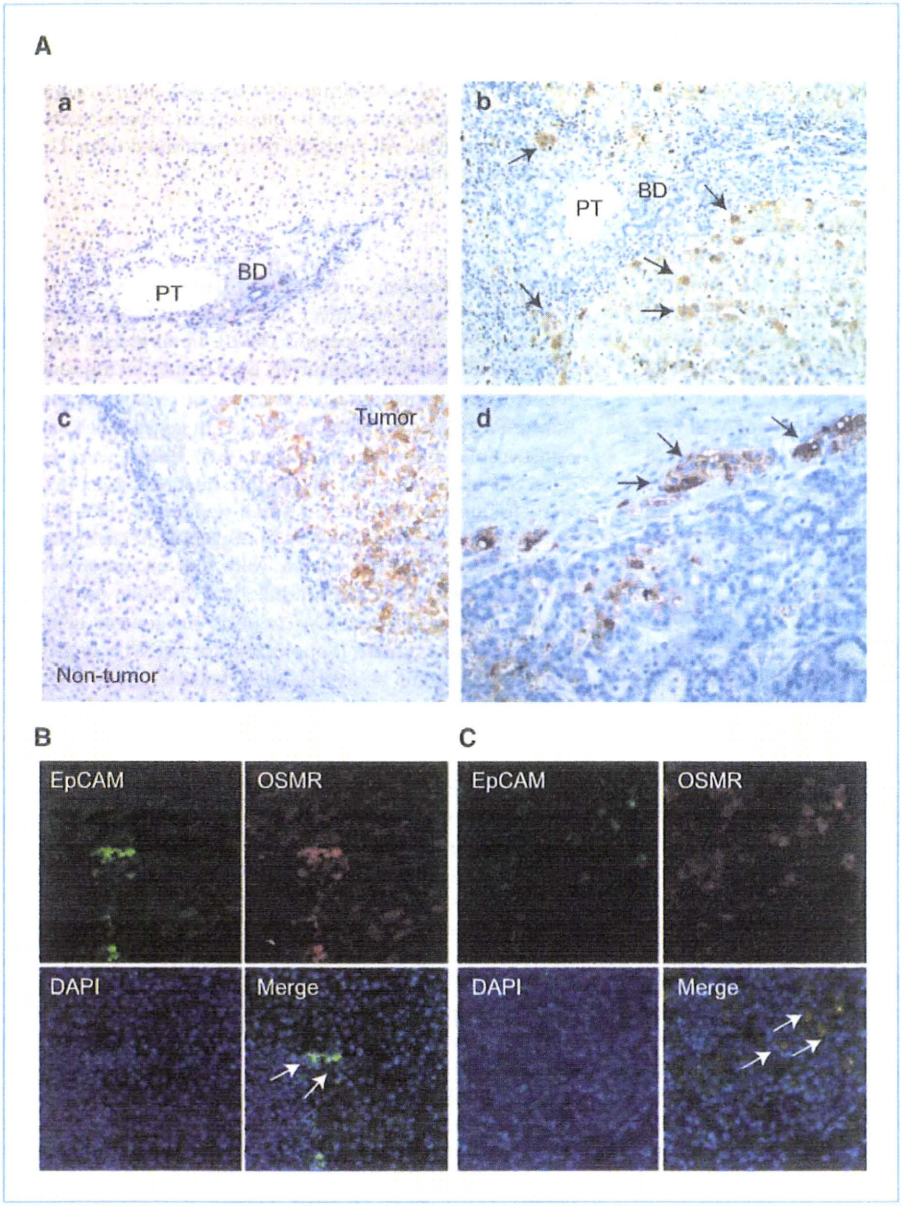

Figure 1. A, representative images of OSMR staining in noncancerous liver tissues and HCC tissues. Immunoreactivity to OSMR was not detected in hepatocytes in chronic hepatitis liver tissue (a) but was detected in a subset of small hepatocyte-like cells in the stroma or transitional cells in the lobule (b, arrows) of cirrhotic liver tissue. OSMR was more abundantly expressed in HCC than in noncancerous liver (c). OSMR$^+$ cancer cells were disseminated in the invasive front area of the tumor (d, arrows). PT, portal tract; BD, bile duct. B and C, double immunofluorescence analysis of EpCAM (green) and OSMR (red) expression in noncancerous (B) and HCC (C) tissues.

(Fig. 2A). Both gp130 and OSMR protein expressions were detected in these cells, consistent with the immunohistochemical data. Because OSM is known to induce the hepatocytic differentiation of hepatoblasts in a STAT3-dependent manner, we investigated the effect of OSM on phosphorylation of STAT3 in HuH1 and HuH7 cells by immunofluorescence and Western blotting. Incubation of HCC cells for 1 hour with OSM at a concentration of 100 ng/mL resulted in the induction and nuclear accumulation of phosphorylated STAT3 compared with controls (Fig. 2B and C). We examined the effect of OSM on the EpCAM$^+$ cell population in HuH1 and HuH7 cells. We first labeled HuH1 and HuH7 cells with CD326 (EpCAM) MicroBeads and FITC-conjugated anti-EpCAM antibodies (Clone Ber-EP4) and performed positive/negative selection using magnetic activated cell sorting to determine the appropriate gating criteria for EpCAM-high (designated as EpCAM$^+$) and EpCAM-low/negative (designated as EpCAM$^-$) cell population (Fig. 2D, top). It is interesting that OSM treatment (100 ng/mL for 72 hours) diminished the EpCAM$^+$ cell population from 50.7% to 10.1% in HuH1 and from 55.2% to 28.8% in HuH7 cells when the same constant gating criteria was applied (Fig. 2D, bottom).

We used RNA interference to investigate whether the decrease in EpCAM$^+$ cells by OSM treatment depends on the expression of OSMR. Transfection of siRNAs specific to *OSMR* (si-OSMR) resulted in the knockdown of target genes

Published OnlineFirst May 18, 2010; DOI:10.1158/0008-5472.CAN-09-4210

compared with the control (si-Control) in HuH1 and HuH7 cells 48 hours after transfection (Supplementary Fig. S2A). We further confirmed the decrease of OSMR protein expression by immunofluorescence and Western blotting 72 hours after transfection (Supplementary Fig. S2B and C). When we treated these HuH1 and HuH7 cells with OSM (100 ng/mL) for 1 hour, we observed the decrease of phosphorylated STAT3 by *OSMR* gene silencing compared with the control (Supplementary Fig. S2C). Furthermore, OSM-mediated decrease in the number of EpCAM$^+$ cells was inhibited by *OSMR* gene silencing (Supplementary Fig. S2D), suggesting that OSM exploits the diminution of EpCAM$^+$ cells through the activation of the OSMR signaling pathway in EpCAM$^+$ HCC.

We further examined the effect of OSM on hepatocytic differentiation by quantitative reverse transcription-PCR and fluorescence-activated cell sorting (FACS) analyses. OSM treatment in HuH1 cells reduced the expression of hepatic progenitor–related genes including *AFP, KRT19* (encoding CK19), and *TERT* (encoding telomerase reverse transcriptase; TERT; Fig. 3A). OSM treatment further reduced the expression of *BMI1* and *POU5F1* (encoding Oct4), which is known to be expressed and required for self-renewal in embryonic stem cells. OSM treatment also increased the expression of the hepatocyte marker, *CYP3A4*. Furthermore, OSM treatment reduced AFP$^+$ and CK19$^+$ cells and increased albumin$^+$ cells compared with the untreated controls, as evaluated by the geometric mean of the fluorescence intensities of whole cells analyzed by intracellular FACS (Fig. 3B). Similar results were obtained in HuH7 cells (data not shown) and, taken together, these data suggest that OSM induced the hepatocytic differentiation of EpCAM$^+$ HCCs.

Hepatocytic differentiation of EpCAM+ HCC by OSM augments cell proliferation

In general, normal stem cells are more quiescent than differentiated cells in terms of cell division. We therefore evaluated the effect of OSM on cell proliferation in HuH1 and HuH7 cells. It is interesting that OSM treatment for 10 days resulted in a larger colony formation following treatment with OSM (100 ng/mL) compared with untreated controls. Of note, the majority of cells comprising these larger colonies were EpCAM$^-$, or had low expression levels, whereas a subset of untreated control cells maintained high EpCAM expression (Fig. 3C). Similar results were obtained when cell proliferation was examined using a [3-(4, 5-dimethylthiazol-2-yl)-5-(3-carboxymethoxyphenyl)-2-(4-sulfophenyl)-2H-tetrazolium] tetrazolium assay and Ki-67 labeling index (Fig. 3D). OSM modestly enhanced cell proliferation (top) and increased Ki-67–positive cells (middle and bottom) compared with untreated controls in both HuH1 and HuH7 cells with statistical significance (Fig. 3D).

OSM treatment increases chemosensitivity of EpCAM+ HCC

The abovementioned data imply that although OSM may induce the hepatocytic differentiation of dormant EpCAM$^+$ liver CSCs, OSM treatment alone might instead enhance cell proliferation through expansion of amplifying differentiated cancer cells *in vitro*, raising the question of efficacy of differentiation therapy in EpCAM$^+$ HCC. Because rapidly amplifying cells are considered to be more sensitive to chemotherapeutic agents, we investigated the effect of combining OSM treatment with conventional chemotherapy to target both dormant CSCs and amplifying non-CSCs. We have shown that 5-FU treatment

Table 1. Clinicopathologic characteristics of OSMR$^+$ and OSMR$^-$ HCC cases used for immunohistochemical analyses

Variables	OSMR$^+$ (n = 66)	OSMR$^-$ (n = 41)	P^*
Age (years, mean ± SE)	62.7 ± 1.3	66.4 ± 1.3	0.052
Sex (male/female)	55/11	27/14	0.058
Etiology (HBV/HCV/other)	25/35/6	8/30/3	0.10
Liver cirrhosis (yes/no)	43/23	26/15	1.0
AFP (ng/mL, mean ± SE)	6,453 ± 5901	1,039 ± 935	0.009
Histologic grade†			
I–II	3	16	
II–III	54	20	
III–IV	9	5	<0.0001
Tumor size (<3 cm/>3 cm)	30/36	15/26	0.42
Tumor-node-metastasis classification			
I/II	48	31	
III/IV	18	10	0.82
EpCAM (positive/negative)	29/37	9/32	0.024

*Mann-Whitney U test or χ^2 test.
†Edmondson-Steiner.

Published OnlineFirst May 18, 2010; DOI:10.1158/0008-5472.CAN-09-4210

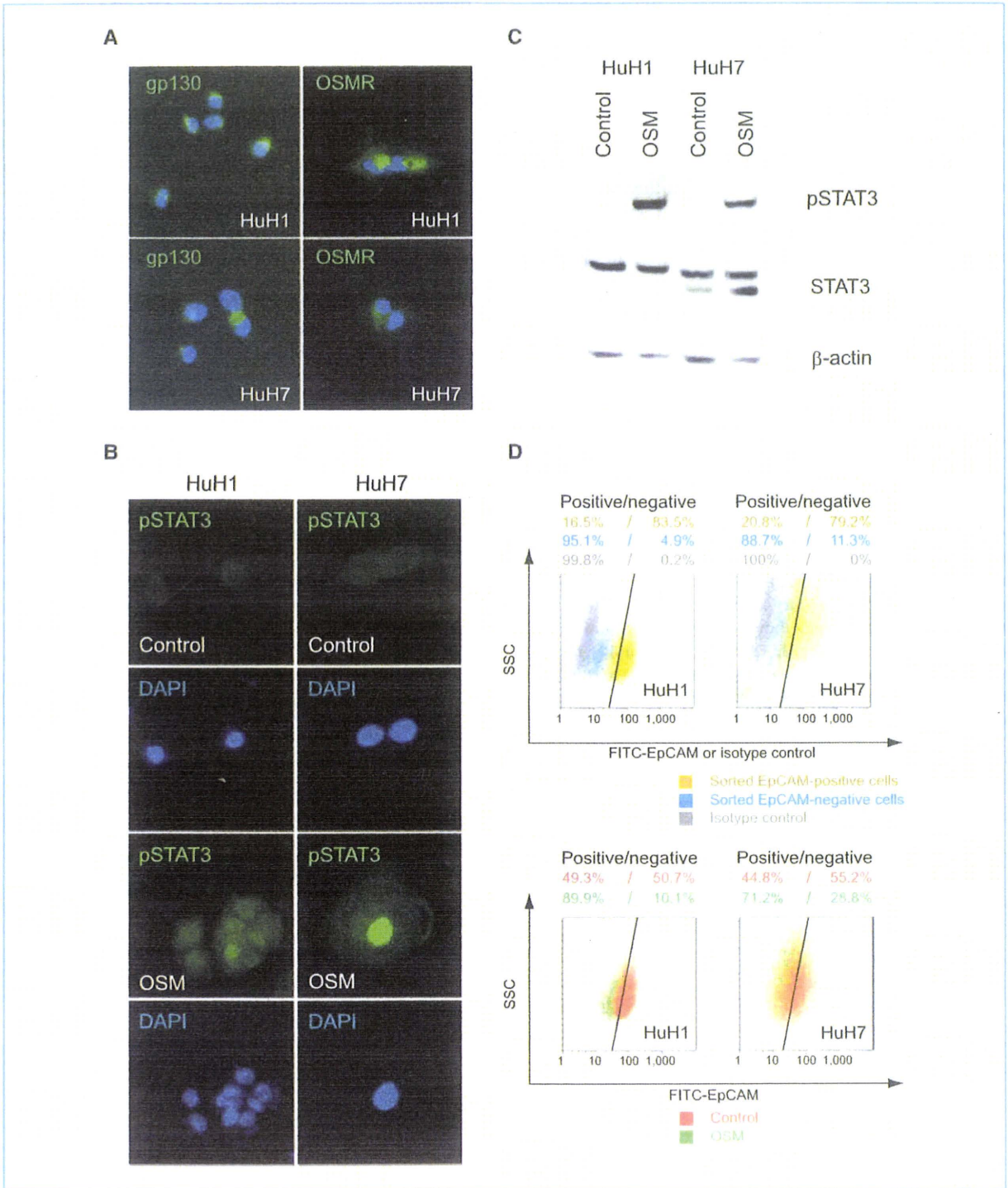

Figure 2. A, immunofluorescence analysis of gp130 and OSMR expression in HuH1 and HuH7 cell lines. B, immunofluorescence analysis of phosphorylated STAT3 expression in HuH1 and HuH7 cell lines stimulated by OSM (100 ng/mL for 1 hour) and controls. C, Western blotting analysis of whole or phosphorylated STAT3 protein expression in HuH1 and HuH7 cells stimulated by OSM (100 ng/mL for 1 hour) and controls. D, FACS analysis of HuH1 and HuH7 cells stained with FITC-conjugated anti-EpCAM antibodies. Top, EpCAM-high (designated as EpCAM$^+$; yellow) and EpCAM-low/negative cells (designated as EpCAM$^-$; blue) were enriched by magnetic activated cell sorting and labeled with FITC-conjugated anti-EpCAM antibodies or isotype control antibodies. Bottom, cells were cultured in 1% FBS DMEM with (green) or without OSM (100 ng/mL; orange) for 3 days and stained with FITC-conjugated anti-EpCAM antibodies.

Published OnlineFirst May 18, 2010; DOI:10.1158/0008-5472.CAN-09-4210

alone could diminish EpCAM⁻ non-CSCs which results in the enrichment of EpCAM⁺ CSCs in HCC (18). We therefore explored the effect of 5-FU in combination with OSM on EpCAM⁺ HCC cell proliferation and apoptosis *in vitro*.

When HuH1 and HuH7 cells were treated with OSM alone and cultured for 7 days, cell proliferation was modestly increased compared with untreated controls (Fig. 4A). In contrast, 5-FU treatment clearly inhibited cell proliferation.

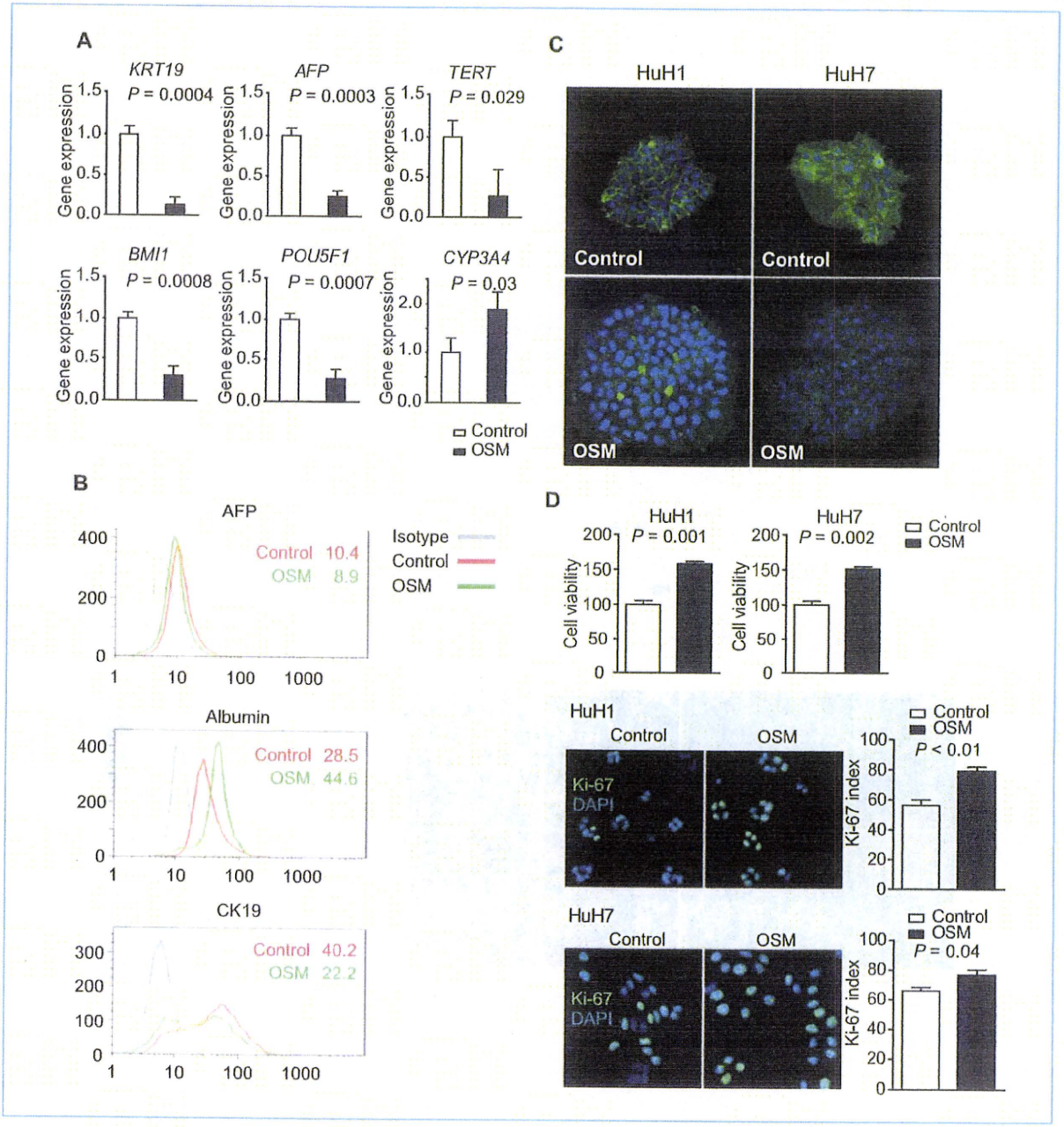

Figure 3. A, quantitative reverse transcription-PCR analysis of HuH1 cells cultured in 1% FBS DMEM with (black columns) or without (white columns) OSM (100 ng/mL) for 3 days. B, intracellular FACS analysis of HuH1 cells cultured in 1% FBS DMEM with (green line) or without (red line) OSM (100 ng/mL) for 3 days. The number in the figure indicates the geometric mean of the fluorescence intensity on a logarithmic scale. C, immunofluorescence analysis of HuH1 and HuH7 cell colonies cultured in 1% FBS DMEM with or without OSM (100 ng/mL) for 10 days. Colonies were fixed with 100% ice-cold methanol and stained with FITC-conjugated anti-EpCAM antibodies. D, top, cell proliferation assay of HuH1 and HuH7 cells cultured in 1% FBS DMEM with (black column) or without (white column) OSM (100 ng/mL) for 3 days. Middle and bottom, immunofluorescence analysis of HuH1 and HuH7 cells cultured in 1% FBS DMEM with or without OSM (100 ng/mL) for 3 days. Cells were fixed with 100% ice-cold methanol and stained with anti–Ki-67 antibodies.

Published OnlineFirst May 18, 2010; DOI:10.1158/0008-5472.CAN-09-4210

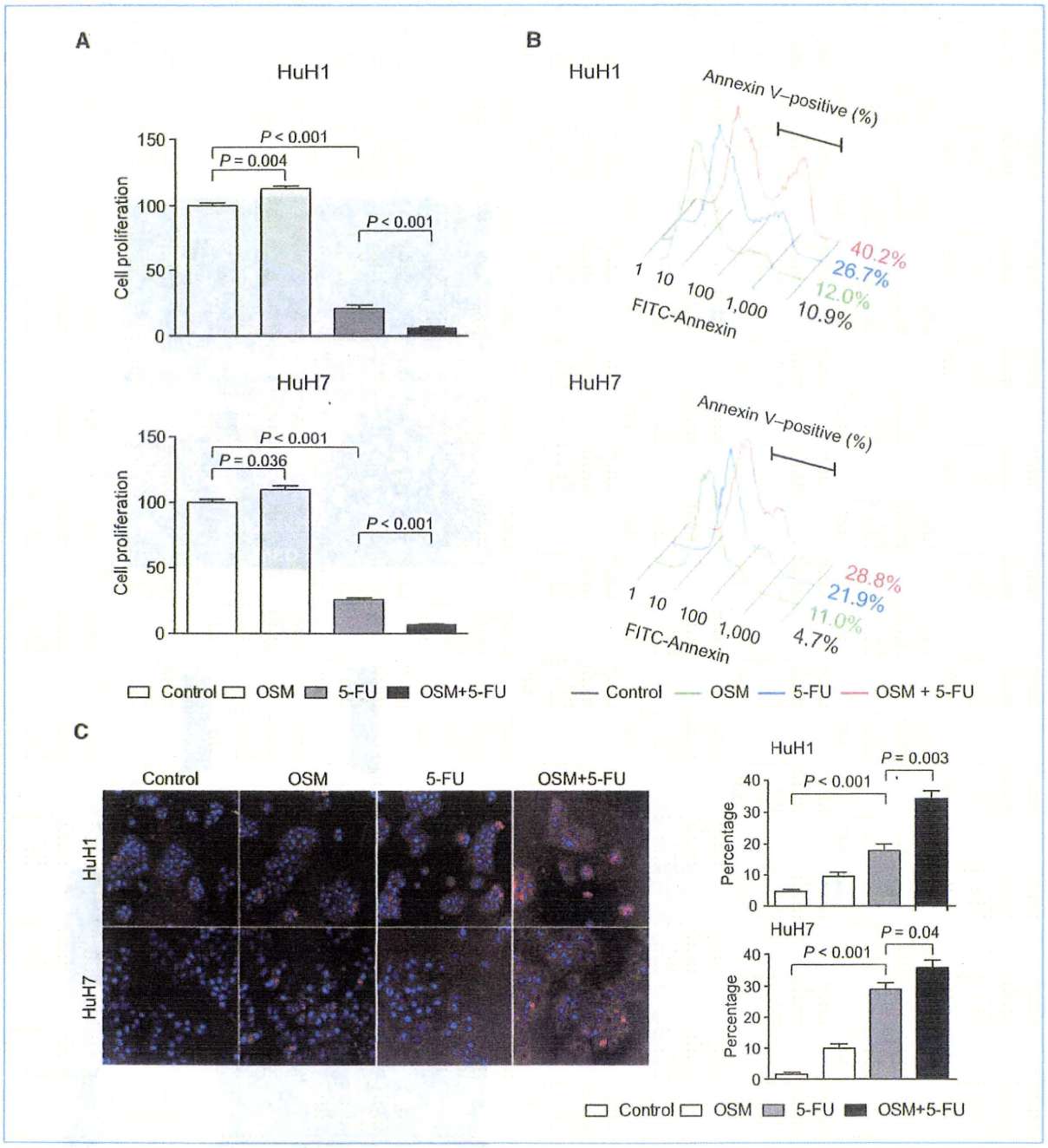

Figure 4. A, cell proliferation assay of HuH1 and HuH7 cells cultured in 1% FBS DMEM with OSM (100 ng/mL; light gray columns), 5-FU (2 μg/mL; gray columns), OSM (100 ng/mL) and 5-FU (2 μg/mL; black columns), or PBS as control (white columns) for 7 days. B, FACS analysis of HuH1 and HuH7 cells stained with FITC-conjugated anti–Annexin V antibodies. Cells were cultured in 1% FBS DMEM with OSM (100 ng/mL; green line), 5-FU (2 μg/mL; blue line), OSM (100 ng/mL) and 5-FU (2 μg/mL; red line), or PBS as control (gray line) for 3 days. C, left, immunofluorescence analysis of HuH1 and HuH7 cells stained with anti–active caspase 3 antibodies. Cells were cultured in 1% FBS DMEM with OSM (100 ng/mL), 5-FU (2 μg/mL), OSM (100 ng/mL) and 5-FU (2 μg/mL), or PBS control for 3 days. Right, bar graphs indicating the percentages of active caspase 3–positive cells.

Noticeably, the combination of OSM and 5-FU effectively suppressed cell proliferation in HuH1 and HuH7 cells (Fig. 4A). We further investigated the effects of OSM and 5-FU on apoptosis, evaluated by Annexin V binding to cell membranes and the activation of caspase 3 (Fig. 4B and C). Although OSM treatment alone had a small effect on the induction of apoptosis, 5-FU treatment induced Annexin V^+ and activated caspase 3^+ cells more than in the control. The

Published OnlineFirst May 18, 2010; DOI:10.1158/0008-5472.CAN-09-4210

combination of OSM and 5-FU most strongly induced apoptosis in both HuH1 and HuH7 cells with statistical significance.

Finally, we investigated the effect of OSM on EpCAM+ HCC *in vivo* using a primary HCC specimen and cell lines. Single-cell suspensions from primary EpCAM+ HCC cells (1×10^6 cells) were injected into 6-week-old male NOD/SCID mice, and these cells formed subcutaneous tumors 48 days after transplantation. Subsequently, 50 μL of PBS, OSM (2 μg/tumor), 5-FU (250 μg/tumor), or OSM (2 μg/tumor) and 5-FU (250 μg/tumor) solution were injected directly into each tumor twice a week. Although OSM treatment alone showed weak tumor-suppressive effects, the changes in tumor size showed no significant difference compared with controls (Fig. 5A). Similarly, 5-FU treatment alone showed limited tumor-suppressive effects. However, the combination of OSM with 5-FU showed a marked inhibition of tumor growth compared with PBS control or 5-FU alone ($P = 0.02$ and 0.05, respectively). Immunohistochemical analysis of xenografted tumors showed that OSM treatment decreased the number of EpCAM+ or CK19+ cells and increased CYP3A4+ cells *in vivo* (Supplementary Fig. S3A and B). FACS analysis of xenografted tumors further confirmed the decrease of EpCAM+ cell population by OSM treatment *in vivo* (Supplementary Fig. S3C). Immunohistochemical analysis revealed that the combination of OSM with 5-FU strongly induced the activation of caspase 3 compared with PBS control, OSM, or 5-FU (Fig. 5B). Taken together, these data suggest that hepatocytic differentiation of EpCAM+ HCC cells induced by OSM was the most effective for inhibition of tumor growth *in vivo* when the conventional chemotherapeutic agent 5-FU was coadministered.

Discussion

A growing body of evidence suggests that there are similarities between normal stem cells and CSCs in terms of self-renewal programs (29). We have recently reported that Wnt/β-catenin signaling augments self-renewal and inhibits the differentiation of EpCAM+ liver CSCs (18). In the present study, we have shown that the OSM-OSMR signaling pathway is maintained in HCCs with stem/progenitor cell features. OSM induces hepatocytic differentiation and activates cell division in dormant EpCAM+ liver CSCs (Fig. 5C). Furthermore, we have shown that the combination of OSM and 5-FU effectively inhibits tumor cell growth, revealing the importance of targeting both CSCs and non-CSCs for eradication of the tumor.

OSM is a pleiotropic cytokine that belongs to the IL-6 family which includes IL-6, IL-11, and leukemia-inhibitory factor. These cytokines share the gp130 receptor subunit as a common signal transducer, and activate Janus tyrosine kinases and the STAT3 pathway. However, gp130 forms a heterodimer with a unique partner such as the IL-6 receptor, leukemia-inhibitory factor receptor, or OSMR, thus transducing a certain signaling uniquely induced by each cytokine (30). Of note, OSM is known to activate hepatocytic differentiation programs in hepatoblasts in an OSMR-specific manner (27), and our data showed that OSM could induce hepatocytic differentiation and active cell proliferation in EpCAM+ HCC through OSMR signaling.

OSMR is expressed in hepatoblasts in the fetal liver (26). We have found that OSMR is frequently expressed in normal hepatic progenitors but is rarely detected in hepatocytes in adult livers. Interestingly, OSMR+ HCC was characterized by

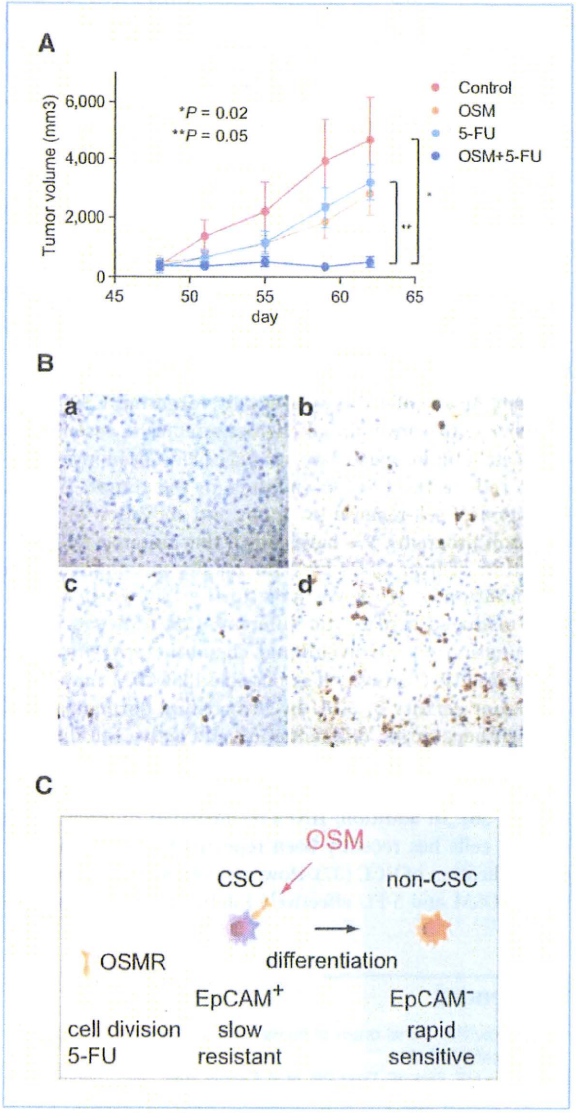

Figure 5. A, effect of PBS, OSM, 5-FU, and OSM plus 5-FU injections on the growth of primary EpCAM+ AFP+ HCC xenograft tumors in NOD/SCID mice ($n = 4$ in each group). Intratumoral injection of 50 μL of PBS, OSM (2 μg/tumor), 5-FU (250 μg/tumor), or OSM (2 μg/tumor) and 5-FU (250 μg/tumor) was initiated 48 days after transplantation, twice per week. B, representative images of activated caspase 3 staining of xenograft tumors in each treatment group (a, PBS; b, OSM; c, 5-FU; and d, OSM and 5-FU). C, a schematic diagram of the effect of OSM on EpCAM+ liver CSCs. Dormant EpCAM+ liver CSCs with OSMR expression respond to OSM and differentiate into rapidly dividing EpCAM- non-CSCs that are highly sensitive to 5-FU.

Published OnlineFirst May 18, 2010; DOI:10.1158/0008-5472.CAN-09-4210

high serum AFP, frequent EpCAM positivity, and poorly differentiated morphology, suggesting that OSMR is more likely expressed in HCC with stem/progenitor cell features (16). Although the regulatory mechanisms of OSMR are still unclear, it is plausible that OSMR expression is regulated by a signaling pathway activated during the process of hepatogenesis. Because gp130 is known to be ubiquitously expressed, regulation of OSM signaling might be largely dependent on the expression status of OSMR in normal and tumor tissues. Recent studies have shown the potential role of methylation of CpG islands located in OSMR promoter in colorectal cancer (31, 32). Clarification of OSMR promoter activity regulation, including CpG methylation, might provide clues for better understanding of hepatocytic differentiation signaling in both normal hepatic stem cells and CSCs.

It has been postulated that both normal stem cells and CSCs are dormant and show slow cell cycles. Consistent with this, CSCs are considered to be more resistant to chemotherapeutic agents than non-CSCs, possibly due to slow cell cycles as well as an increased expression of ATP-binding cassette transporters, robust DNA damage responses, and activated antiapoptotic signaling (20, 33, 34). Therefore, development of an effective strategy by targeting CSC pools together with conventional chemotherapies is essential to eradicate a tumor mass. Two strategies have been investigated to reduce the CSCs population in the tumor; that is, inhibition of self-renewal programs and activation of differentiation programs. We have shown that hepatocytic differentiation of liver CSCs by OSM results in enhanced cell proliferation *in vitro*. We have further shown here that OSM-mediated hepatocytic differentiation of liver CSCs in combination with conventional chemotherapy effectively suppresses HCC growth. It is possible that OSM may boost antitumor activity of 5-FU by "exhausting dormant CSCs" through hepatocytic differentiation and active cell division. It is encouraging that similar success with differentiation therapy has recently been reported in several cancers (24, 35, 36). In addition, HNF4-α–mediated differentiation of HCC cells has recently been reported to be effective for the eradication of HCC (37). However, although the combination of OSM and 5-FU effectively inhibited tumor growth in our model, we could not observe the shrinkage of the tumor. Thus, induction of CSC's differentiation with eradication of non-CSCs might not be enough for the eradication of the tumor, which might suggest the importance of inhibiting self-renewal as well as stimulating differentiation of CSCs. Because we induced the hepatocytic differentiation of the subcutaneous tumor by local injection of OSM, further rigorous studies are clearly required to assess the effect of OSM on liver CSCs and its utility for differentiation therapy in HCC.

CSCs may acquire resistance against differentiation therapy by additional genetic/epigenetic changes during treatment by clonal evolution, as observed in conventional chemotherapy. Indeed, it has recently been suggested that bone morphogenetic protein–mediated brain CSC differentiation failed in a subset of brain tumors in which bone morphogenetic protein receptor promoters were methylated and silenced (23). Similarly, OSMR silencing by promoter methylation might result in the development of OSM-resistant clones in HCC.

In conclusion, OSMR is expressed in certain types of HCC with stem/progenitor cell features, and OSM induces hepatocytic differentiation and active cell division of $OSMR^+$ liver CSCs to enhance chemosensitivity to 5-FU. The clinical safety and utility of OSM should be evaluated in the near future.

Disclosure of Potential Conflicts of Interest

No potential conflicts of interest were disclosed.

Acknowledgments

We thank Masayo Baba and Nami Nishiyama for excellent technical assistance.

Grant Support

Ministry of Education, Culture, Sports, Science and Technology, Japan grant-in-aid (no. 20599005).

The costs of publication of this article were defrayed in part by the payment of page charges. This article must therefore be hereby marked *advertisement* in accordance with 18 U.S.C. Section 1734 solely to indicate this fact.

Received 11/17/2009; revised 03/12/2010; accepted 03/31/2010; published OnlineFirst 05/18/2010.

References

1. Fialkow PJ. Clonal origin of human tumors. Biochim Biophys Acta 1976;458:283–321.
2. Clarke MF, Dick JE, Dirks PB, et al. Cancer stem cells—perspectives on current status and future directions: AACR Workshop on Cancer Stem Cells. Cancer Res 2006;66:9339–44.
3. Jordan CT, Guzman ML, Noble M. Cancer stem cells. N Engl J Med 2006;355:1253–61.
4. Al-Hajj M, Wicha MS, Benito-Hernandez A, Morrison SJ, Clarke MF. Prospective identification of tumorigenic breast cancer cells. Proc Natl Acad Sci U S A 2003;100:3983–8.
5. Bonnet D, Dick JE. Human acute myeloid leukemia is organized as a hierarchy that originates from a primitive hematopoietic cell. Nat Med 1997;3:730–7.
6. O'Brien CA, Pollett A, Gallinger S, Dick JE. A human colon cancer cell capable of initiating tumour growth in immunodeficient mice. Nature 2007;445:106–10.
7. Ricci-Vitiani L, Lombardi DG, Pilozzi E, et al. Identification and expansion of human colon-cancer-initiating cells. Nature 2007; 445:111–5.
8. Singh SK, Hawkins C, Clarke ID, et al. Identification of human brain tumour initiating cells. Nature 2004;432:396–401.
9. Visvader JE, Lindeman GJ. Cancer stem cells in solid tumours: accumulating evidence and unresolved questions. Nat Rev Cancer 2008;8:755–68.
10. El-Serag HB, Rudolph KL. Hepatocellular carcinoma: epidemiology and molecular carcinogenesis. Gastroenterology 2007;132: 2557–76.
11. Mishra L, Banker T, Murray J, et al. Liver stem cells and hepatocellular carcinoma. Hepatology 2009;49:318–29.
12. Chiba T, Kita K, Zheng YW, et al. Side population purified from hepatocellular carcinoma cells harbors cancer stem cell-like properties. Hepatology 2006;44:240–51.

Published OnlineFirst May 18, 2010; DOI:10.1158/0008-5472.CAN-09-4210

13. Ma S, Chan KW, Hu L, et al. Identification and characterization of tumorigenic liver cancer stem/progenitor cells. Gastroenterology 2007;132:2542–56.
14. Yang ZF, Ho DW, Ng MN, et al. Significance of CD90+ cancer stem cells in human liver cancer. Cancer Cell 2008;13:153–66.
15. Yang W, Yan HX, Chen L, et al. Wnt/β-catenin signaling contributes to activation of normal and tumorigenic liver progenitor cells. Cancer Res 2008;68:4287–95.
16. Yamashita T, Forgues M, Wang W, et al. EpCAM and α-fetoprotein expression defines novel prognostic subtypes of hepatocellular carcinoma. Cancer Res 2008;68:1451–61.
17. Yamashita T, Budhu A, Forgues M, Wang XW. Activation of hepatic stem cell marker EpCAM by Wnt-β-catenin signaling in hepatocellular carcinoma. Cancer Res 2007;67:10831–9.
18. Yamashita T, Ji J, Budhu A, et al. EpCAM-positive hepatocellular carcinoma cells are tumor-initiating cells with stem/progenitor cell features. Gastroenterology 2009;136:1012–24.
19. Boman BM, Huang E. Human colon cancer stem cells: a new paradigm in gastrointestinal oncology. J Clin Oncol 2008;26:2828–38.
20. Dean M, Fojo T, Bates S. Tumour stem cells and drug resistance. Nat Rev Cancer 2005;5:275–84.
21. Zou GM. Cancer initiating cells or cancer stem cells in the gastrointestinal tract and liver. J Cell Physiol 2008;217:598–604.
22. Hill RP, Perris R. "Destemming" cancer stem cells. J Natl Cancer Inst 2007;99:1435–40.
23. Lee J, Son MJ, Woolard K, et al. Epigenetic-mediated dysfunction of the bone morphogenetic protein pathway inhibits differentiation of glioblastoma-initiating cells. Cancer Cell 2008;13:69–80.
24. Piccirillo SG, Reynolds BA, Zanetti N, et al. Bone morphogenetic proteins inhibit the tumorigenic potential of human brain tumour-initiating cells. Nature 2006;444:761–5.
25. Nasr R, Guillemin MC, Ferhi O, et al. Eradication of acute promyelocytic leukemia-initiating cells through PML-RARA degradation. Nat Med 2008;14:1333–42.
26. Kamiya A, Kinoshita T, Ito Y, et al. Fetal liver development requires a paracrine action of oncostatin M through the gp130 signal transducer. EMBO J 1999;18:2127–36.
27. Kinoshita T, Miyajima A. Cytokine regulation of liver development. Biochim Biophys Acta 2002;1592:303–12.
28. Yamashita T, Honda M, Takatori H, et al. Activation of lipogenic pathway correlates with cell proliferation and poor prognosis in hepatocellular carcinoma. J Hepatol 2009;50:100–10.
29. Lobo NA, Shimono Y, Qian D, Clarke MF. The biology of cancer stem cells. Annu Rev Cell Dev Biol 2007;23:675–99.
30. Heinrich PC, Behrmann I, Haan S, Hermanns HM, Muller-Newen G, Schaper F. Principles of interleukin (IL)-6-type cytokine signalling and its regulation. Biochem J 2003;374:1–20.
31. Deng G, Kakar S, Okudiara K, Choi E, Sleisenger MH, Kim YS. Unique methylation pattern of oncostatin m receptor gene in cancers of colorectum and other digestive organs. Clin Cancer Res 2009; 15:1519–26.
32. Kim MS, Louwagie J, Carvalho B, et al. Promoter DNA methylation of oncostatin m receptor-β as a novel diagnostic and therapeutic marker in colon cancer. PLoS One 2009;4:e6555.
33. Bao S, Wu Q, McLendon RE, et al. Glioma stem cells promote radioresistance by preferential activation of the DNA damage response. Nature 2006;444:756–60.
34. Viale A, De Franco F, Orleth A, et al. Cell-cycle restriction limits DNA damage and maintains self-renewal of leukaemia stem cells. Nature 2009;457:51–6.
35. Gupta PB, Onder TT, Jiang G, et al. Identification of selective inhibitors of cancer stem cells by high-throughput screening. Cell 2009; 138:645–59.
36. Sipkins DA. Rendering the leukemia cell susceptible to attack. N Engl J Med 2009;361:1307–9.
37. Yin C, Lin Y, Zhang X, et al. Differentiation therapy of hepatocellular carcinoma in mice with recombinant adenovirus carrying hepatocyte nuclear factor-4α gene. Hepatology 2008;48:1528–39.

Genomics 95 (2010) 217–223

Contents lists available at ScienceDirect

Genomics

journal homepage: www.elsevier.com/locate/ygeno

Comprehensive gene expression analysis of 5′-end of mRNA identified novel intronic transcripts associated with hepatocellular carcinoma

Yuji Hodo [a], Shin-ichi Hashimoto [b], Masao Honda [a], Taro Yamashita [a], Yutaka Suzuki [c], Sumio Sugano [c], Shuichi Kaneko [a,*], Kouji Matsushima [b]

[a] Department of Gastroentelorogy, Kanazawa University Graduate School of Medical Science, 13-1 Takara-Machi, Kanazawa, Ishikawa 920-8641, Japan
[b] Department of Molecular Preventive Medicine, School of Medicine, The University of Tokyo, 7-3-1, Hongo, Bunkyo-ku, Tokyo 113-0033, Japan
[c] Department of Medical Genome Sciences, Graduate School of Frontier Sciences, The University of Tokyo, 5-1-5, Kashiwanoha, Kashiwa, Chiba 277-8562, Japan

ARTICLE INFO

Article history:
Received 1 June 2009
Accepted 14 January 2010
Available online 21 January 2010

Keywords:
5′-end serial analysis of gene expression
Transcriptional start site
Acyl-coenzyme A oxidase 2
Intron
Hepatocellular carcinoma

ABSTRACT

To elucidate the molecular feature of human hepatocellular carcinoma (HCC), we performed 5′-end serial analysis of gene expression (5′SAGE), which allows genome-wide identification of transcription start sites in addition to quantification of mRNA transcripts. Three 5′SAGE libraries were generated from normal human liver (NL), non-B, non-C HCC tumor (T), and background non-tumor tissues (NT). We obtained 226,834 tags from these libraries and mapped them to the genomic sequences of a total of 8,410 genes using RefSeq database. We identified several novel transcripts specifically expressed in HCC including those mapped to the intronic regions. Among them, we confirmed the transcripts initiated from the introns of a gene encoding acyl-coenzyme A oxidase 2 (*ACOX2*). The expression of these transcript variants were up-regulated in HCC and showed a different pattern compared with that of ordinary *ACOX2* mRNA. The present results indicate that the transcription initiation of a subset of genes may be distinctively altered in HCC, which may suggest the utility of intronic RNAs as surrogate tumor markers.

Introduction

Hepatocellular carcinoma (HCC) is the fifth most common cancer worldwide and the third most common cause of cancer mortality. HCC usually develops in patients with virus-induced (e.g., hepatitis B virus (HBV) and hepatitis C virus (HCV)) chronic inflammatory liver disease [1]; however, non-B, non-C HCC has been reported in patients negative for both HBV and HCV [2]. HCC development is a multistep process involving changes in host gene expression, some of which are correlated with the appearance and progression of a tumor. Multiple studies linking hepatitis viruses and chemical carcinogens with hepatocarcinogesis have provided insights into tumorigenesis [1,3]. Nevertheless, the genetic events that lead to HCC development remain unknown, and the molecular pathogenesis of HCC in most patients is still unclear. Therefore, elucidation of the genetic changes specific to the pathogenesis of non-B, non-C HCC may be useful to reveal the molecular features of HCCs irrelevant to viral infection.

Gene expression profiling, either by cDNA microarray [4] or serial analysis of gene expression (SAGE) [5], is a powerful molecular technique that allows analysis of the expression of thousands of genes. In particular, SAGE enables the rapid, quantitative, and simultaneous monitoring of the expression of tens of thousands of genes in various tissues [6,7]. Although numerous studies using cDNA microarrays and SAGE have been performed to clarify the genomic and molecular alterations associated with HCC [6,8–10], most expression data have been derived from the 3′-end region of mRNA. Recent advances in molecular biology have enabled genome-wide analysis of the 5′-end region of mRNA that revealed the variation in transcriptional start sites [11,12] and the presence of a large number of non-coding RNAs [13]. These approaches might be useful for identifying the unique and undefined genes associated with HCC not identified by the analysis of the 3′-end region of mRNA. SAGE based on the 5′-end (5′SAGE), a recently developed technique, allows for a comprehensive analysis of the transcriptional start site and quantitative gene expression [14]. This article is to elucidate the molecular carcinogenesis of non-B, non-C HCCs, while those heterogeneous entities are supposed not to share the same etiology, by using 5′SAGE.

Results

Annotation of the 5′SAGE tags to the human genome

We characterized a total of 226,834 tags from three unique 5′SAGE libraries (75,268 tags from the normal liver (NL) library, 75,573 tags from the non-tumor tissue (NT) library, and 75,993 tags from the tumor (T) library) and compared them against the human genome

Abbreviations: 5′SAGE, 5′-end serial analysis of gene expression; HCC, hepatocellular carcinoma; ACOX2, acyl-coenzyme A oxidase 2.

* Corresponding author. Fax: +81 76 234 4250
E-mail address: skaneko@m-kanazawa.jp (S. Kaneko).

0888-7543/$ – see front matter © 2010 Elsevier Inc. All rights reserved.
doi:10.1016/j.ygeno.2010.01.004

sequence. A total of 211,818 tags matched genomic sequences, representing 104,820 different tags in the three libraries (Table 1). About 60–65% of these tags mapped to a single locus in the genome in each library. Then, we mapped these single-matched tags to the well-annotated genes using RefSeq database (www.ncbi.nlm.nih.gov/RefSeq/, reference sequence database developed by NCBI). A total of 45,601 tags from the NL library, 39,858 from the NT library, and 41,265 from the T library were successfully mapped to 8410 unique genes (4397 genes detected in the NL library, 5194 genes in the NT library, and 6304 genes in the T library).

Gene expression profiling of non-B, non-C HCC

Abundantly expressed transcripts in the NL library and their corresponding expression in the NT and T libraries are shown in Table 2. The most abundant transcript in all three libraries was encoded by the *albumin (ALB)* gene. Transcripts encoding apolipoproteins were also abundantly expressed in each library, suggesting the preservation of hepatocytic gene expression patterns in HCC. Of note, the expression of *haptoglobin (HP)* (NL: 631, NT: 329, T: 57) and *metallothionein 1G (MT1G)* (NL: 392, NT: 169, T: 2) was decreased in the NT library and more in T library compared with NL library. Furthermore, the expression of *metallothionein 2A (MT2A)* (NL: 1027, NT: 872, T: 19), *metallothionein 1X (MT1X)* (NL: 547, NT: 644, T: 11), and *metallothionein 1E (MT1E)* (NL: 275, NT: 340, T: 2) was decreased almost fifty-fold or more in the T library compared with the NL and NT libraries. In contrast, the expression of *ribosomal protein S29 (RPS29)* (NL: 372, NT: 1011, T: 1768) was increased in the NT library and more in T library compared with NL library. Thus, transcripts associated with a certain liver function including xenobiotic metabolism might be suppressed whereas those associated with protein synthesis might be expressed in non-B, non-C HCC, similar to that observed in HCV-HCC [15].

We then investigated the characteristics of gene expression patterns in non-B, non C HCC. Two hundred fifty-four and 172 genes were up- or down-regulated in the T library more than five-fold compared with the NL library (data not shown). The top 10 genes are listed in Table 3a, and we identified several novel genes not yet reported to be differentially expressed in non-B, non-C HCC. Representative novel gene expression changes identified by 5′SAGE were validated by semi-quantitative reverse transcriptase-polymerase chain reaction (RT-PCR) analysis (Supplemental Fig. 1). RT-PCR results showed that the expression of *galectin 4 (LGALS4)*, *X antigen family, member 1A (XAGE 1A)*, *retinol dehydrogenase 11 (RDH11)*, *hydroxysteroid (17-beta) dehydrogenase 14 (HSD17B14)* *transmembrane 14A (TMEM14A)*, *stimulated by retinoic acid 13 homolog (STRA13)*, and *dual specificity phosphatase 23 (DUSP23)* was increased, whereas the expression of *C-type lectin superfamily 4 member G (CLEC4G)* was decreased in HCC tissues compared with the non-tumor tissues.

To further characterize the gene expression patterns of non-B, non-C HCC comprehensively, we compared the Gene Ontology process of three types of HCCs (i.e., non-B, non-C HCC; HBV-HCC; HCV-HCC) based on our previously described data [16]. The pathway analysis using MetaCore™ software showed that the immune related and cell adhesion related pathways were up-regulated in HCV-HCC with statistically significance, and the insulin signaling and angiogenesis related pathways were up-regulated in HBV-HCC with statistically significance, confirming our previous results [16]. Interestingly, genes associated with progesterone signaling were up-regulated in non-B, non-C HCC, while genes associated with proteolysis in the cell cycle, apoptosis and the ESR1-nuclear pathway were up-regulated in all types of HCC (Supplemental Fig. 2).

Dynamic alteration of transcription initiation in HCC

Although various transcriptome analyses have discovered considerable gene expression changes in cancer, it is still unclear if transcription is differentially initiated and/or terminated in HCC compared with the non-cancerous liver. We therefore explored the characteristics of transcription initiation and/or termination in HCC using 5′SAGE and 3′SAGE data. Markedly, we observed relevant differences between 5′ SAGE and 3′SAGE data derived from the same HCC sample (Tables 3a and b). For example, a gene encoding *coagulation factor XIII, B polypeptide (F13B)* was 13-fold up-regulated at transcription start sites (5′SAGE) but two-fold down-regulated at transcription termination sites (3′SAGE). On the other hand, a gene encoding *adenylate cyclase 1 (ADCY1)* was 50-fold down-regulated at transcriptional termination sites (3′SAGE) but showed no difference at transcriptional start sites (5′SAGE). These data suggest the dramatic alteration of all process of transcription in HCC, and the transcripts initiated at certain sites might be specifically associated with and involved in HCC pathogenesis, which could be a novel marker for HCC diagnosis.

Identification of novel intronic transcripts in HCC

Recent lines of evidence suggest that the majority of sequences of eukaryotic genomes may be transcribed, not only from known transcription start sites but also from intergenic regions and introns [17,18]. Introns are recognized as a significant source of functional non-coding RNAs (ncRNAs) including microRNAs (miRNAs) [18]. Moreover, a recent report implied the role of some large intronic RNAs in the pathogenesis of several types of malignancies [19]. Thus, analysis of transcripts originating from introns might be valuable for elucidating the genetic traits of HCC. We therefore focused on the transcriptional start sites potentially initiated from the intron and deregulated in HCC using 5′SAGE data. We identified that 97% of 5′ SAGE tags annotated by the RefSeq database matched the sequences in the exons, while 3% matched those in the introns (1257 in the N library, 1225 in the NT library, and 1261 in the T library) (Table 4a). To identify the possible promoter regions located in the intron, we clustered the different SAGE tags to a certain genomic region if these tags positioned within 500 bp intervals (Supplemental Fig. 3), as described previously [12].

Table 1
Experimental matching of 5′SAGE tags to genome.

	Normal liver	Non-tumor	Tumor	Total
All tags	75,268	75,573	75,993	226,834
Tags mapped to genome (%)				
1 locus/genome	51,076 (71.2)	47,200 (68.0)	48,503 (68.5)	146,779 (69.3)
Multiple loci/genome	20,608 (28.8)	22,142 (32.0)	22,289 (31.5)	65,039 (30.7)
Total tags	71,684 (100)	69,342 (100)	70,792 (100)	211,818 (100)
Unique tags mapped to genome (%)				
1 locus/genome	20,736 (65.5)	20,487 (60.2)	23,753 (60.7)	64,976 (62.0)
Multiple loci/genome	10,914 (34.5)	13,548 (39.8)	15,382 (39.3)	39,844 (38.0)
Total tags	31,650 (100)	34,035 (100)	39,135 (100)	104,820 (100)
Total tags to RefSeq	45,601	39,858	41,265	126,724
Unique gene	4397	5194	6304	8410

5′SAGE indicates 5′-end serial analysis of gene expression.

Table 2
The highly expressed genes in the NL library and corresponding expression in the NT and T libraries (top 50 from NL library).

Tag count			Ratio		Gene
NL	NT	T	NT/NL	T/NL	
3731	1716	2328	0.460	0.624	Albumin (ALB)
2484	2146	2042	0.864	0.822	Apolipoprotein C-I (APOC1)
1955	1603	1079	0.820	0.552	Apolipoprotein A-II (APOA2)
1653	1050	828	0.635	0.501	Apolipoprotein A-I (APOA1)
1252	1908	1203	1.524	0.961	Transthyretin (prealbumin, amyloidosis type I) (TTR)
1233	724	220	0.587	0.178	Serpin peptidase inhibitor, clade A, member 1 (SERPINA1)
1027	872	19	0.849	0.019	Metallothionein 2A (MT2A)
755	1144	762	1.515	1.009	Ferritin, light polypeptide (FTL)
713	632	680	0.886	0.954	Alpha-1-microglobulin/bikunin precursor (AMBP)
635	524	1336	0.825	2.104	Apolipoprotein E (APOE)
631	329	57	0.521	0.090	Haptoglobin (HP)
600	228	212	0.380	0.353	Fibrinogen gamma chain (FGG)
549	395	302	0.719	0.550	Apolipoprotein C-III (APOC3)
547	644	11	1.177	0.020	Metallothionein 1X (MT1X)
479	257	290	0.537	0.605	Tumor protein, translationally-controlled 1 (TPT1)
463	217	53	0.469	0.114	Serpin peptidase inhibitor, clade A, member 3 (SERPINA3)
393	204	206	0.519	0.524	Ribosomal protein L26 (RPL26)
392	169	2	0.431	0.005	Metallothionein 1G (MT1G)
372	1011	1768	2.718	4.753	Ribosomal protein S29 (RPS29)
306	163	223	0.533	0.729	Ribosomal protein S27 (RPS27)
279	135	159	0.484	0.570	Ribosomal protein S16 (RPS16)
275	340	2	1.236	0.007	Metallothionein 1E (MT1E)
269	170	246	0.632	0.914	Ribosomal protein S23 (RPS23)
260	142	92	0.546	0.354	Fibrinogen beta chain (FGB)
260	200	195	0.769	0.750	Aldolase B, fructose-bisphosphate (ALDOB)
255	228	286	0.894	1.122	Ribosomal protein S12 (RPS12)
248	162	198	0.653	0.798	Ribosomal protein S14 (RPS14)
246	175	70	0.711	0.285	Interferon induced transmembrane protein 3 (IFITM3)
239	198	273	0.828	1.142	Ribosomal protein L31(RPL31)
229	264	0	1.153	0.004	Hepcidin antimicrobial peptide (HAMP)
228	149	156	0.654	0.684	Ribosomal protein S20 (RPS20)
222	191	117	0.860	0.527	Ubiquitin B (UBB)
216	218	352	1.009	1.630	Ribosomal protein L41 (RPL41)
210	150	155	0.714	0.738	Ribosomal protein, large, P1(RPLP1)
201	110	90	0.547	0.448	Ribosomal protein, large, P2 (RPLP2)
198	102	64	0.515	0.323	Fibrinogen alpha chain (FGA)
196	143	408	0.730	2.082	Ribosomal protein L37 (RPL37)
192	123	56	0.641	0.292	Ribosomal protein L37a (RPL37A)
191	208	346	1.089	1.812	Ribosomal protein L30 (RPL30)
174	109	76	0.626	0.437	Ribosomal protein L35 (RPL35)
169	208	3	1.231	0.018	Cytochrome P450, family 2, subfamily E, polypeptide 1 (CYP2E1)
167	105	300	0.629	1.796	Apolipoprotein H (beta-2-glycoprotein I) (APOH)
162	106	33	0.654	0.204	Serum amyloid A4, constitutive (SAA4)
159	85	157	0.535	0.987	Ribosomal protein L34 (RPL34)
159	113	229	0.711	1.440	Transferrin (TF)
155	84	135	0.542	0.871	Ribosomal protein S11 (RPS11)
152	125	101	0.822	0.664	Ribosomal protein S13 (RPS13)
147	84	1	0.571	0.007	Nicotinamide *N*-methyltransferase (NNMT)
147	180	35	1.224	0.238	Hemopexin (HPX)
146	89	121	0.610	0.829	Alpha-2-HS-glycoprotein (AHSG)

To avoid division by 0, a tag value of 1 for any tag that was not detectable was used.
NL, normal liver; NT, non-tumor; T, tumor.

More than 2 tags were detected in the intronic regions of the 164 genes in the NL, 168 genes in the NT, and 157 genes in the T library, suggesting that these regions might be potential intronic promoter regions (Table 4a). The biological process of these intron-origin transcripts using Human Protein Reference Database (http://www.hprd.org/) showed that these were related to basic cellular functions such as signal transduction, transport, and regulation of the nucleobase and nucleotide, suggesting that these intronic transcripts may play a fundamental role in the liver (data not shown). Among these genes, 12 were differentially expressed between the NL and T libraries more than four-fold (Table 4b). Interestingly, intronic transcripts (determined by 5′SAGE) of genes encoding *SAMD3*,

Table 3a
Differently expressed genes in HCC (top 10 from 5′SAGE).

5′SAGE	3′SAGE	5′/3′	Gene
T/NL	T/NL	Ratio	
Up-regulated gene			
19	6	3.17	P antigen family, member 2 (prostate associated) (PAGE2)
18	10	1.8	Lectin, galactoside-binding, soluble, 4 (LGALS4)
16	3	5.33	Choline phosphotransferase 1 (CHPT1)
14	2	7	X antien family, member 1A (XAGE1A)
14	2	7	Dehydrogenase/reductase (SDR family) member 4 (DHRS4)
14	2	7	Sterol-C5-desaturase-like (SC5DL)
13	0.5	26	Coagulation factor XIII, B polypeptide (F13B)
13	2.33	5.58	Retinol dehydrogenase 11 (all-trans and 9-cis) (RDH11)
13	0.5	26	Transmembrane protein 14A (TMEM14A)
12	1.33	9.02	Dual specificity phosphatase 23 (DUSP23)
Down-regulated gene			
0.00436	0.0137	0.318	Hepcidin antimicrobial peptide (HAMP)
0.0051	ND		Metallothionein 1G (MT1G)
0.0068	0.04	0.17	Nicotinamide *N*-methyltransferase (NNMT)
0.00727	ND		Metallothionein 1E (functional) (MT1E)
0.0098	0.0526	0.186	C-reactive protein, pentraxin-related (CRP)
0.0145	ND		Metallothionein 1 M (MT1M)
0.0152	ND		Phospholipase A2, group IIA (platelets, synovial fluid) (PLA2G2A)
0.0178	0.111	0.16	Cytochrome P450, family 2, subfamily E, polypeptide 1 (CYP2E1)
0.0185	0.192	0.096	Metallothionein 2A (MT2A)
0.0201	ND		Metallothionein 1X (MT1X)

3′SAGE, 3′-end serial analysis of gene expression; 5′SAGE, 5′-end serial analysis of gene expression; HCC, hepatocellular carcinoma; NL, normal liver; T, tumor.

Table 3b
Differently expressed genes in HCC (top 10 from 3′SAGE).

5′SAGE	3′SAGE	5′/3′	Gene
T/NL	T/NL	Ratio	
Up-regulated gene			
ND	15		Leukocyte immunoglobulin-like receptor, subfamily B, member 1 (LILRB1)
ND	12		Fibroblast growth factor 5 (FGF5)
1	11	0.909	Adenosine deaminase, tRNA-specific 1 (ADAT1)
5	11	0.454	px19-like protein (PRELID1)
4.4	11	0.4	Anaphase promoting complex subunit 11 (ANAPC11)
ND	10.3		Chromosome 21 open reading frame 77 (C21orf77)
ND	10		von Willebrand factor (VWF)
2.333	10	0.233	ATX1 antioxidant protein 1 homolog (yeast) (ATOX1)
18	10	1.8	Lectin, galactoside-binding, soluble, 4 (LGALS4)
ND	9.5		Solute carrier family 26 (sulfate transporter), member 2 (SLC26A2)
Down-regulated gene			
0.5	0.012	41.7	ELL associated factor 1 (EAF1)
0.5	0.0137	36.5	TGF beta-inducible nuclear protein 1 (NSA2)
0.000436	0.0137	0.032	Hepcidin antimicrobial peptide (HAMP)
1	0.0179	55.9	Basic, immunoglobulin-like variable motif containing (BIVM)
ND	0.0182		DNA fragmentation factor, 45 kDa, alpha polypeptide (DFFA)
1	0.0185	54.1	GRIP1 associated protein 1 (GRIPAP1)
ND	0.0189		Nuclear factor of activated T-cells 5, tonicity-responsive (NFAT5)
1	0.0204	49	Adenylate cyclase 1 (ADCY1)
0.333	0.0312	10.7	Dihydroorotate dehydrogenase (DHODH)
0.738	0.0312	23.7	Ribosomal protein, large, P1 (RPLP1)

3′SAGE, 3′-end serial analysis of gene expression; 5′SAGE, 5′-end serial analysis of gene expression; HCC, hepatocellular carcinoma; NL, normal liver; T, tumor.

Table 4a
Number of 5′SAGE tags mapped to intronic region.

	NL	NT	T
Tag mapped to intron	1287	1253	1292
Total promoter region	952	981	1020
(tag number = 1)	788	813	863
(tag number ≧2)	164	168	157

ACOX2, *HGD*, *CYP3A5*, *KNG1* and *AGXT* were increased, while their 3′ transcripts (determined by 3′SAGE) were decreased in HCC. In contrast, both 5′ intronic transcripts and 3′ transcripts encoding *HFM1*, *SERPINA1*, *SUPT3H*, *A2M* and *TMEM176B* were similarly decreased in HCC. Taken together, these data imply that the canonical- and intronic-promoter activities of a subset of genes including *SAMD3*, *ACOX2*, *HGD*, *CYP3A5*, *KNG1* and *AGXT* might be differently regulated in HCC.

ACOX2 as a novel intronic gene deregulated in HCC

A subset of genes listed above may be transcribed from intronic regions specifically in HCC. Among these genes, we focused on the regulation of *ACOX2*, which is reported to be potentially involved in peroxisomal beta-oxidation and hepatocarcinogenesis [20]. The intron-origin expression of *ACOX2* increased six-fold in HCC compared with the NT by 5′SAGE, while the expression based on the 3′end was almost similar between HCC and NT lesions (Table 4b). Close examination of 5′SAGE data identified two potential intron-origin transcripts of *ACOX2* (Supplemental Fig. 4). The first (intronic-*ACOX2-1*) was initiated upstream of the tenth exon, whereas the second (intronic-*ACOX2-2*) was initiated upstream of the twelfth exon of *ACOX2* (Supplemental Fig. 4). The sequence of the intronic part was unique, and the remaining part of the sequence was shared with the canonical transcripts of *ACOX2*.

The expression of canonical *ACOX2* and the two types of intron-origin transcripts was investigated in NL, NT, and T tissues by RT-PCR (Fig. 1A). Although canonical *ACOX2* expression was decreased in T than in NL, the intron-origin transcript, particularly intronic-*ACOX2-1*, was increased in T. Intronic-*ACOX2-2* transcripts also showed a modest increase. We further evaluated the alteration of these transcripts in 19 HBV-HCCs, 20 HCV-HCCs, and 4 non-B, non-C HCCs, and their background liver tissues by canonical *ACOX2* and intronic-*ACOX2* specific real-time detection (RTD)-PCR. Although the expression of canonical *ACOX2* was decreased, the expression of intronic-*ACOX2* was significantly increased (Fig. 1B). Importantly, the gene expression ratios of intronic-to canonical *ACOX2* increased more in moderately differentiated HCCs (mHCC) than in well-differentiated HCCs (wHCC), suggesting the involvement of intronic-*ACOX2* expression on HCC progression.

Table 4b
Differentially expressed intronic promoter regions in HCC.

5′SAGE T/NL	3′SAGE T/NL	5′/3′ Ratio	Gene
Up-regulated			
9	1	9.00	Sterile alpha motif domain containing 3 (SAMD3)
6	0.89	6.74	Acyl-Coenzyme A oxidase 2, branched chain (ACOX2)
6	0.62	9.68	Homogentisate 1,2-dioxygenase (homogentisate oxidase) (HGD)
6	0.009	666.67	Cytochrome P450, family 3, subfamily A, polypeptide 5 (CYP3A5)
5	0.64	7.81	Kininogen 1 (KNG1)
4	0.36	11.11	Alanine-glyoxylate aminotransferase (AGXT)
4	1	4.00	Crystallin, alpha A (CRYAA)
Down-regulated			
0.13	1	0.13	HFM1, ATP-dependent DNA helicase homolog (*S. cerevisiae*) (HFM1)
0.25	0.51	0.49	Serpin peptidase inhibitor, clade A member 1 (SERPINA1)
0.25	1	0.25	Suppressor of Ty 3 Homolog (*S. cerevisiae*) (SUPT3H)
0.25	0.2	1.25	Alpha-2-macroglobulin (A2M)
0.25	0.083	3.13	Transmembrane protein 176B (TMEM176B)

3′SAGE, 3′-end serial analysis of gene expression; 5′SAGE, 5′-end serial analysis of gene expression; HCC, hepatocellular carcinoma; NL, normal liver; NT, non-tumor; T, tumor.

Discussion

This is the first comprehensive transcriptional analysis of tissue lesions of non-B, non-C HCC, background liver and NL using the 5′ SAGE method. Approximately 6.7% of our 5′SAGE tags showed no matching within the human genome, possibly due to the presence of a single nucleotide polymorphism (SNP) in the human genome. Out of the complete matched tags in the genome, 70% were assigned to unique positions and 30% to two or more loci. The tags with multiple matches with genomic loci were largely retrotransposon elements, repetitive sequences, and pseudogenes.

In this study, the analysis of non-B, non-C HCC enabled us to evaluate direct molecular changes associated with HCC without any bias of gene induction by virus infection. The gene expression profile based on our 5′SAGE tags revealed that *albumin (ALB)* and apolipoproteins were highly expressed in NL, indicating the massive production of plasma proteins in NL; these results are similar to those of our previous study using 3′SAGE [6]. Other genes such as *aldolase B (ALDOB)*, *antitrypsin (SERPINA1)*, and *haptoglobin (HP)* were also highly expressed in NL, in both the 5′SAGE and 3′SAGE libraries (Table 2) [6]. Comparison of the expression profiles among NL, background NT and T identified several differentially expressed transcripts in T. *Galectin-4 (LGALS4)* was up-regulated and *HAMP*, *NNMT*, *CYP2E1*, and *metallothionein* were down-regulated in HCC in accordance with previous findings (Table 3a) [8,9,21]. Moreover, *CLEC4G*, which was predominantly expressed in the sinusoidal endothelial cells of the liver, was down-regulated in HCC. In addition, we first found that *P antigen family, member 2 (PAGE2)* and *XAGE1A* were up-regulated in HCC (Table 3a, Supplemental Fig. 1). These genes were members of cancer-testis antigen that include MAGE-family genes. MAGE-family members were originally found to be up-regulated in HCV-related HCC, and reported to be useful as molecular markers and as possible target molecules for immunotherapy in human HCC [22]. In this study, we identified that these members of genes were also up-regulated in non B, non-C HCC. Thus, these genes may be useful as molecular markers and therapeutic targets for the treatment of a certain type of human HCC.

There existed some discrepancy between 5′SAGE and 3′SAGE results, even though they were derived from the same sample. Technical issues such as amplication error, difference of restriction enzyme, and annotation error have been described previously [14]. It is possible that 3′ transcripts might be more stable than 5′ transcripts by binding of ribosomal proteins during translation. Another possibility is the diversity of the transcriptional start and/or termination sites. One of the advantages of 5′SAGE analysis is the potential to determine the transcriptional start sites in each gene. Indeed, a recent study indicated the importance of an insulin splice variant in the pathogenesis of insulinomas [23]. Considering the diversity of 5′ends of genes, it is more appropriate to perform 5′SAGE in combination with 3′SAGE when determining the frequency of gene expression and identifying novel transcript variants.

Here, we were able to identify at least 12 intron-origin transcripts that were differentially expressed in HCC compared with the background liver or NL. These transcripts could not be identified by the 3′SAGE approach. We also performed detailed expression analysis of *ACOX2* that was involved in the beta-oxidation of peroxisome. We

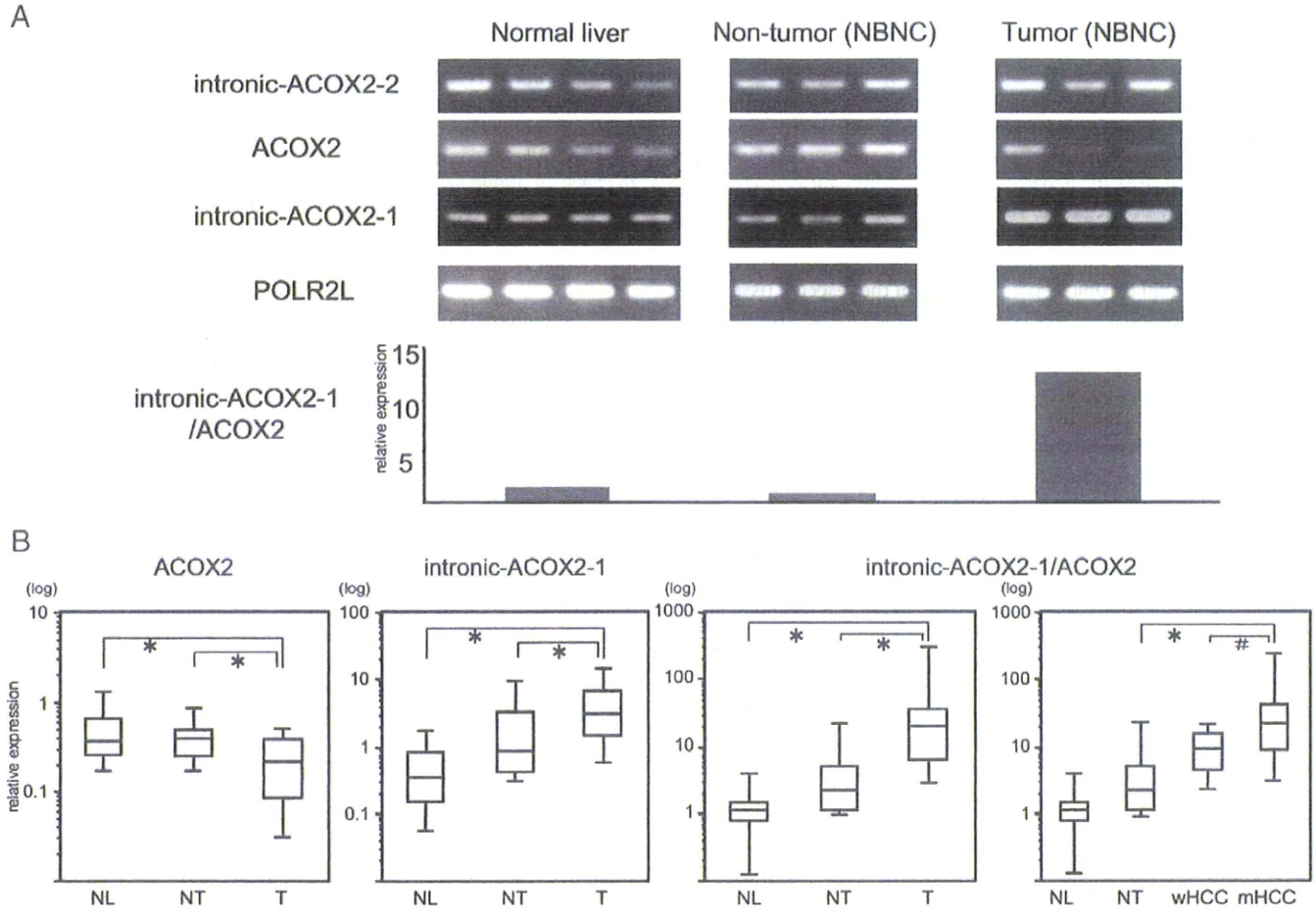

Fig. 1. (A) RT-PCR results of *ACOX2* and *ACOX2* intronic RNAs in independent NL, NT (non-B, non-C), and T (non-B, non-C) samples. RT-PCR was performed in triplicate for each sample-primer set from cDNA. The PCR products were semi-quantitatively analyzed with ImageJ software and calculated as levels relative to *polymerase (RNA) II (DNA directed) polypeptide L (POLR2L)*. The bar graph indicates the expression ratio of intronic-ACOX2-1 to canonical ACOX2. The expression pattern of intron 1 was different from that of canonical *ACOX2*. (B) RTD-PCR analysis of *ACOX2* and *ACOX2* intronic RNAs in NL, T (HBV-related, HCV-related, and non-B, non-C), and NT tissues. Quantitative RTD-PCR was performed in duplicate for each sample-primer set from cDNA. Each sample was normalized relative to *POLR2L*. All HCC tissues were pathologically diagnosed as well differentiated HCC (wHCC) or moderately differentiated HCC (mHCC). Kruskal–Wallis tests and Mann–Whitney *U* tests were used for statistical analysis. ACOX2, acyl-Coenzyme A oxidase 2; HCC, hepatocellular carcinoma; NL, normal liver; NT, non-tumor; RT-PCR, reverse transcriptase-polymerase chain reaction; RTD-PCR, real-time detection-PCR; T, tumor. $^{*}P<0.01$, $\#P<0.05$.

were able to clone the intron-origin *ACOX2* RNAs (intronic-*ACOX2-1, 2*) for the first time and found that intronic-*ACOX2-1* was significantly overexpressed in T compared with NT and NL. The ratio of intronic-*ACOX2-1* and canonical *ACOX2* (relative intronic-*ACOX2*) was progressively up-regulated from NL via the background liver to HCC. Importantly, the expression of relative intronic-*ACOX2* was more up-regulated in moderately differentiated HCC than in well-differentiated HCC. The intronic difference in expression might be due to a polymorphism, since the 5′SAGE library for NL and T were from different people. The mechanisms of stepwise increase of intronic-*ACOX2* in the process of hepatocarinogenesis should be clarified in future.

ACOX2 is a rate-limiting enzyme of branched-chain acyl-CoA oxidase involved in the degradation of long branched fatty acid and bile acid intermediates in peroxisomes. *ACOX2* expression was associated with the differentiation state of hepatocytes and was repressed under the undifferentiated phase of human hepatoma cell lines [24]. A decreased *ACOX2* expression was also reported in prostate cancer [25]. Here, the expression of canonical *ACOX2* was decreased, while that of intronic-*ACOX2-1* was increased in HCC. The deduced amino acid of intronic-*ACOX2-1* encodes the C-terminal (from 386 to 681 amino acids) of canonical *ACOX2*, lacking the active sites for FAD binding and a fatty acid as the substrate, suggesting that the protein may be functionally departed [26]. The biological role of the increased intronic-*ACOX2-1* was not clear, but it might be reflected by the activation of peroxisome proliferators-activated receptor alpha (PPARA). It is reported that mice lacking ACOX1, another rate-limiting enzyme in peroxisomal straight-chain fatty acid oxidation, developed steatosis and HCC characterized by increased mRNA and protein expression of genes regulated by PPARα [27]. The importance of PPARα activation in HCC development has been recently reported using HCV core protein transgenic mice [28]. Moreover, the overexpression of alpha-methylacyl-CoA racemase (AMACR), an enzyme for branched-chain fatty acid beta-oxidation, is reported to be a reliable diagnostic marker of prostate cancer and is associated with the decreased expression of ACOX2 [25]. Therefore, the expression of intronic-*ACOX2-1* might open the door for further investigations of their potential clinical use, e.g., serving as diagnostic markers of HCC, although the functional relevance of this gene should be further clarified.

In conclusion, we report the first comprehensive transcriptional analysis of non-B, non-C HCC, NT background liver, and NL tissue, based on 5′SAGE. This study offers new insights into the transcriptional changes that occur during HCC development as well as the molecular mechanism of carcinogenesis in the liver. The results suggest the presence of unique intron-origin RNAs that are useful as diagnostic markers and may be used as new therapeutic targets.

Material and methods

Samples

Samples were obtained from a 56-year-old man who had undergone surgical hepatic resection for the treatment of solitary HCC. Serological tests for hepatitis B surface (HBs) antigen and anti-HCV antibodies were negative. Tumor (T) and non-tumor (NT) tissue samples were separately obtained from the tumorous parts (diagnosed as moderately differentiated HCC) and non-tumorous parts (diagnosed as mild chronic hepatitis: F1A1) of the resected tissue. We also obtained five normal liver (NL) tissue samples from five patients who had undergone surgical hepatic resection because of metastatic liver cancer. None of the patients was seropositive for both HBs antigen and anti-HCV antibodies. Neither heavy alcohol consumption nor the intake of chemical agents was observed before surgical resection. All laboratory values related to hepatic function were within the normal range. All procedures and risks were explained verbally and provided in a written consent form.

We additionally used independent four NL tissue samples, 19 HBV-HCCs, 20 HCV-HCCs and 4 non-B, non-C HCCs, and their background liver tissue samples for reverse transcriptase-polymerase chain reaction (RT-PCR) and real-time detection (RTD)-PCR (Supplemental Table 1). Four non-B, non-C HCCs were histologically diagnosed as moderately differentiated HCCs, and the adjacent non-cancerous liver tissues were diagnosed as a normal liver, a chronic hepatitis, a pre-cirrhotic liver and a cryptogenic liver cirrhosis, respectively. None of the patients was seropositive for HBs antigen, anti-HBs antibodies, anti-hepatitis B core (HBc) antibodies and anti-HCV antibodies. Neither heavy alcohol consumption nor the intake of chemical agents was observed. Histological grading of the tumor was evaluated by two independent pathologists as described previously [16].

Generation of the 5′ SAGE library

5′SAGE libraries were generated as previously described [14]. Five to ten micrograms of poly(A)+RNA was treated with bacterial alkaline phosphatase (BAP; TaKaRa, Otsu, Japan). Poly(A)+RNA was extracted twice with phenol: chloroform (1:1), ethanol precipitated, and then treated with tobacco acid pyrophosphatase (TAP). Two to four micrograms of the BAP-TAP-treated poly(A)+RNA was divided into two aliquots and an RNA linker containing recognition sites for *Eco*RI/*Mme*I was ligated using RNA ligase (TaKaRa): one aliquot was ligated to a 5′-oligo 1 (5′-GGA UUU GCU GGU GCA GUA CAA CGA AUU CCG AC-3′) linker, and the other aliquot was ligated to a 5′-oligo 2 (5′-CUG CUC GAA UGC AAG CUU CUG AAU UCC GAC-3′) linker. After removing unligated 5′-oligo, cDNA was synthesized using RNaseH-free reverse-transcriptase (Superscript II, Invitrogen, Carlsbad, CA, USA) at 12 °C for 1 h and 42 °C for the next hour, using 10 pmol of dT adapter-primer (5′-GCG GCT GAA GAC GGC CTA TGT GGC CTT TTT TTT TTT TTT TTT-3′). After first-strand synthesis, RNA was degraded in 15 mM NaOH at 65 °C for 1 h. cDNA was amplified in a volume of 100 μl by PCR with 16 pmol of 5′ (5′ [biotin]-GGA TTT GCT GGT GCA GTA CAA-3′ or 5′[biotin]-CTG CTC GAA TGC AAG CTT CTG-3′) and 3′ (5′-GCG GCT GAA GAC GGC CTA TGT-3′) PCR primers. cDNA was amplified using 10 cycles at 94 °C for 1 min, 58 °C for 1 min, and 72 °C for 2 min. PCR products were digested with the *Mme*I type IIS restriction endonuclease (NEB, Pickering, Ontario, Canada). The digested 5′-terminal cDNA fragments were bound to streptavidin-coated magnetic beads (Dynal, Oslo, Norway). cDNA fragments that bound to the beads were directly ligated together in a reaction mixture containing T4 DNA ligase in a supplied buffer for 2.5 h at 16 °C. The ditags were amplified by PCR using the following primers: 5′ GGA TTT GCT GGT GCA GTA CA 3′ and 5′ CTG CTC GAA TGC AAG CTT CT 3′. The PCR products were analyzed by polyacrylamide gel electrophoresis (PAGE) and digested with *Eco*RI. The region of the gel containing the ditags was excised and the fragments were self-ligated to produce long concatamers that were then cloned into the *Eco*RI site of pZero 1.0 (Invitrogen). Colonies were screened by PCR using the M13 forward and reverse primers. PCR products containing inserts of more than 600 bp were sequenced with Big Dye terminator ver.3 and analyzed using a 3730 ABI automated DNA sequencer (Applied Biosystems, Foster City, CA, USA). All electrophoretograms were reanalyzed by visual inspection to check for ambiguous bases and to correct misreads. In this study, we obtained 19–20 bp tag information.

Association of the 5′SAGE tags with their corresponding genes

We attempted to align our 5′tags with the human genome (NCBI build 36, available from http://www.genome.ucsc.edu/) using the alignment program ALPS (http://www.alps.gi.k.u-tokyo.ac.jp/). Only tags that matched in sense orientation were considered in our analysis. The RefSeq database was searched for transcripts corresponding to the regions adjacent to the alignment location of each 5′tag.

RT-PCR

Total RNA was extracted using a ToTally RNA extraction kit (Ambion, Inc., Austin, TX, USA). Total RNA (500 ng) was reverse-transcribed in a 100-μl reaction solution containing 240 U of Moloney murine leukemia virus reverse transcriptase (Promega, Madison, WI, USA), 80 U of RNase inhibitor (Promega), 4.6 mM $MgCl_2$, 6.6 mM DTT, 1 mM dNTPs, and 2 mM random hexamer (Promega), at 42 °C for 1 h. PCR was performed in a 20-μl volume containing 0.5 U of AmpliTaq DNA polymerase (Applied Biosystems), 16.6 mM $(NH_4)_2SO_4$, 67 mM Tris–HCl, 6.7 mM $MgCl_2$, 10 mM 2-mercaptoethanol, 1 mM dNTPs, and 1.5 μM sense and antisense primers, using an ABI 9600 thermal cycler (Applied Biosystems). The amplification protocol included 28–30 cycles of 95 °C for 45 s, 58 °C for 1 min, and 72 °C for 1 min. Primer sequences are shown in Supplemental Table 2. RT-PCR was performed in triplicate for each sample-primer set. Each sample was normalized relative to *polymerase (RNA) II (DNA directed) polypeptide L (POLR2L)*. *POLR2L* is a housekeeping gene that showed relatively stable gene expression in various tissues [29]. The PCR products were semi-quantitatively analyzed with ImageJ software (http://rsb.info.nih.gov/ij/).

RTD-PCR

Intron-origin transcript expression was quantified using TaqMan Universal Master Mix (Applied Biosystems). The samples were amplified using an ABI PRISM 7900HT Sequence Detection System (Applied Biosystems). Using the standard curve methods, quantitative PCR was performed in duplicate for each sample-primer set. Each sample was normalized relative to *POLR2L*. The assay IDs used were Hs00185873_m1 for *ACOX2* and Hs00360764_m1 for *POLR2L*. The specific primers and probe sequence of intronic-*ACOX2-1* were 5′-TTCATAAAGTTGTGAGCA-GAGGAAA-3′ (forward), 5′-TGCACCACTTACTGAGCATCTACTC-3′ (reverse), and 5′-ACTTCTTACCTCAGAGCTG-3′ (probe).

Analysis of pathway network

MetaCore™ software (GeneGo Inc., St. Joseph, MI) was used to investigate the molecular pathway networks of non-B, non-C HCC, HBV-HCC and HCV-HCC. All genes up-regulated more than five-fold in all HCC libraries subjected to Enrichment analysis in GO process networks by default settings ($p<0.05$).

Statistical analysis

Kruskal–Wallis tests were used to compare the expression among normal liver, non-cancerous tissues, and HCC tissues. Mann–Whitney *U* tests were also used to evaluate the statistical significance of ACOX2

gene expression levels between two groups. All statistical analyses were performed using R (http://www.r-project.org/).

Acknowledgments

The authors would like to thank Mr. Shungo Deshimaru and Ms. Keiko Harukawa for technical assistance.

Appendix A. Supplementary data

Supplementary data associated with this article can be found, in the online version, at doi:10.1016/j.ygeno.2010.01.004.

References

[1] H.B. El-Serag, K.L. Rudolph, Hepatocellular carcinoma: epidemiology and molecular carcinogenesis, Gastroenterology 132 (2007) 2557–2576.
[2] Y. Yokoi, S. Suzuki, S. Baba, K. Inaba, H. Konno, S. Nakamura, Clinicopathological features of hepatocellular carcinomas (HCCs) arising in patients without chronic viral infection or alcohol abuse: a retrospective study of patients undergoing hepatic resection, J. Gastroenterol. 40 (2005) 274–282.
[3] R.N. Aravalli, C.J. Steer, E.N. Cressman, Molecular mechanisms of hepatocellular carcinoma, Hepatology 48 (2008) 2047–2063.
[4] D.J. Duggan, M. Bittner, Y. Chen, P. Meltzer, J.M. Trent, Expression profiling using cDNA microarrays, Nat. Genet. 21 (1999) 10–14.
[5] V.E. Velculescu, L. Zhang, B. Vogelstein, K.W. Kinzler, Serial analysis of gene expression, Science 270 (1995) 484–487.
[6] T. Yamashita, S. Hashimoto, S. Kaneko, S. Nagai, N. Toyoda, T. Suzuki, K. Kobayashi, K. Matsushima, Comprehensive gene expression profile of a normal human liver, Biochem. Biophys. Res. Commun. 269 (2000) 110–116.
[7] S. Hashimoto, S. Nagai, J. Sese, T. Suzuki, A. Obata, T. Sato, N. Toyoda, H.Y. Dong, M. Kurachi, T. Nagahata, K. Shizuno, S. Morishita, K. Matsushima, Gene expression profile in human leukocytes, Blood 101 (2003) 3509–3513.
[8] H. Okabe, S. Satoh, T. Kato, O. Kitahara, R. Yanagawa, Y. Yamaoka, T. Tsunoda, Y. Furukawa, Y. Nakamura, Genome-wide analysis of gene expression in human hepatocellular carcinomas using cDNA microarray: identification of genes involved in viral carcinogenesis and tumor progression, Cancer. Res. 61 (2001) 2129–2137.
[9] Y. Shirota, S. Kaneko, M. Honda, H.F. Kawai, K. Kobayashi, Identification of differentially expressed genes in hepatocellular carcinoma with cDNA microarrays, Hepatology 33 (2001) 832–840.
[10] T. Yamashita, M. Honda, S. Kaneko, Application of serial analysis of gene expression in cancer research, Curr. Pharm. Biotechnol. 9 (2008) 375–382.
[11] Y. Suzuki, H. Taira, T. Tsunoda, J. Mizushima-Sugano, J. Sese, H. Hata, T. Ota, T. Isogai, T. Tanaka, S. Morishita, K. Okubo, Y. Sakaki, Y. Nakamura, A. Suyama, S. Sugano, Diverse transcriptional initiation revealed by fine, large-scale mapping of mRNA start sites, EMBO Rep. 2 (2001) 388–393.
[12] K. Kimura, A. Wakamatsu, Y. Suzuki, T. Ota, T. Nishikawa, R. Yamashita, J. Yamamoto, M. Sekine, K. Tsuritani, H. Wakaguri, S. Ishii, T. Sugiyama, K. Saito, Y. Isono, R. Irie, N. Kushida, T. Yoneyama, R. Otsuka, K. Kanda, T. Yokoi, H. Kondo, M. Wagatsuma, K. Murakawa, S. Ishida, T. Ishibashi, A. Takahashi-Fujii, T. Tanase, K. Nagai, H. Kikuchi, K. Nakai, T. Isogai, S. Sugano, Diversification of transcriptional modulation: large-scale identification and characterization of putative alternative promoters of human genes, Genome. Res. 16 (2006) 55–65.
[13] T. Shiraki, S. Kondo, S. Katayama, K. Waki, T. Kasukawa, H. Kawaji, R. Kodzius, A. Watahiki, M. Nakamura, T. Arakawa, S. Fukuda, D. Sasaki, A. Podhajska, M. Harbers, J. Kawai, P. Carninci, Y. Hayashizaki, Cap analysis gene expression for high-throughput analysis of transcriptional starting point and identification of promoter usage, Proc. Natl. Acad. Sci. U. S. A. 100 (2003) 15776–15781.
[14] S. Hashimoto, Y. Suzuki, Y. Kasai, K. Morohoshi, T. Yamada, J. Sese, S. Morishita, S. Sugano, K. Matsushima, 5′-end SAGE for the analysis of transcriptional start sites, Nat. Biotechnol. 22 (2004) 1146–1149.
[15] T. Yamashita, S. Kaneko, S. Hashimoto, T. Sato, S. Nagai, N. Toyoda, T. Suzuki, K. Kobayashi, K. Matsushima, Serial analysis of gene expression in chronic hepatitis C and hepatocellular carcinoma, Biochem. Biophys. Res. Commun. 282 (2001) 647–654.
[16] T. Yamashita, M. Honda, H. Takatori, R. Nishino, H. Minato, H. Takamura, T. Ohta, S. Kaneko, Activation of lipogenic pathway correlates with cell proliferation and poor prognosis in hepatocellular carcinoma, J. Hepatol. 50 (2009) 100–110.
[17] J.S. Mattick, Introns: evolution and function, Curr. Opin. Genet. Dev. 4 (1994) 823–831.
[18] J.S. Mattick, I.V. Makunin, Non-coding RNA, Hum. Mol. Genet. 15 (Spec No 1) (2006) R17–29.
[19] R. Louro, A.S. Smirnova, S. Verjovski-Almeida, Long intronic noncoding RNA transcription: expression noise or expression choice? Genomics 93 (2009) 291–298.
[20] S. Yu, S. Rao, J.K. Reddy, Peroxisome proliferator-activated receptors, fatty acid oxidation, steatohepatitis and hepatocarcinogenesis, Curr. Mol. Med. 3 (2003) 561–572.
[21] N. Kondoh, T. Wakatsuki, A. Ryo, A. Hada, T. Aihara, S. Horiuchi, N. Goseki, O. Matsubara, K. Takenaka, M. Shichita, K. Tanaka, M. Shuda, M. Yamamoto, Identification and characterization of genes associated with human hepatocellular carcinogenesis, Cancer. Res. 59 (1999) 4990–4996.
[22] Y. Kobayashi, T. Higashi, K. Nouso, H. Nakatsukasa, M. Ishizaki, T. Kaneyoshi, N. Toshikuni, K. Kariyama, E. Nakayama, T. Tsuji, Expression of MAGE, GAGE and BAGE genes in human liver diseases: utility as molecular markers for hepatocellular carcinoma, J. Hepatol. 32 (2000) 612–617.
[23] A.H. Minn, M. Kayton, D. Lorang, S.C. Hoffmann, D.M. Harlan, S.K. Libutti, A. Shalev, Insulinomas and expression of an insulin splice variant, Lancet 363 (2004) 363–367.
[24] H. Stier, H.D. Fahimi, P.P. Van Veldhoven, G.P. Mannaerts, A. Volkl, E. Baumgart, Maturation of peroxisomes in differentiating human hepatoblastoma cells (HepG2): possible involvement of the peroxisome proliferator-activated receptor alpha (PPAR alpha), Differentiation 64 (1998) 55–66.
[25] S. Zha, S. Ferdinandusse, J.L. Hicks, S. Denis, T.A. Dunn, R.J. Wanders, J. Luo, A.M. De Marzo, W.B. Isaacs, Peroxisomal branched chain fatty acid beta-oxidation pathway is upregulated in prostate cancer, Prostate 63 (2005) 316–323.
[26] K. Tokuoka, Y. Nakajima, K. Hirotsu, I. Miyahara, Y. Nishina, K. Shiga, H. Tamaoki, C. Setoyama, H. Tojo, R. Miura, Three-dimensional structure of rat-liver acyl-CoA oxidase in complex with a fatty acid: insights into substrate-recognition and reactivity toward molecular oxygen, J. Biochem. 139 (2006) 789–795.
[27] K. Meyer, Y. Jia, W.Q. Cao, P. Kashireddy, M.S. Rao, Expression of peroxisome proliferator-activated receptor alpha, and PPARalpha regulated genes in spontaneously developed hepatocellular carcinomas in fatty acyl-CoA oxidase null mice, Int. J. Oncol. 21 (2002) 1175–1180.
[28] N. Tanaka, K. Moriya, K. Kiyosawa, K. Koike, F.J. Gonzalez, T. Aoyama, PPARalpha activation is essential for HCV core protein-induced hepatic steatosis and hepatocellular carcinoma in mice, J. Clin. Invest. 118 (2008) 683–694.
[29] C. Rubie, K. Kempf, J. Hans, T. Su, B. Tilton, T. Georg, B. Brittner, B. Ludwig, M. Schilling, Housekeeping gene variability in normal and cancerous colorectal, pancreatic, esophageal, gastric and hepatic tissues, Mol. Cell. Probes. 19 (2005) 101–109.

Liver INTERNATIONAL
OFFICIAL JOURNAL OF THE INTERNATIONAL ASSOCIATION FOR THE STUDY OF THE LIVER

Liver International ISSN 1478-3223

CLINICAL STUDIES

dUTP pyrophosphatase expression correlates with a poor prognosis in hepatocellular carcinoma

Hajime Takatori[1], Taro Yamashita[1], Masao Honda[1], Ryuhei Nishino[1], Kuniaki Arai[1], Tatsuya Yamashita[1], Hiroyuki Takamura[2], Tetsuo Ohta[2], Yoh Zen[3] and Shuichi Kaneko[1]

1 Department of Gastroenterology, Kanazawa University Graduate School of Medical Science, Ishikawa, Japan
2 Department of Gastroenterologic Surgery, Kanazawa University Graduate School of Medical Science, Ishikawa, Japan
3 Pathology Section, Kanazawa University Hospital, Ishikawa, Japan

Keywords
dUTP pyrophosphatase – hepatocellular carcinoma – prognosis – serial analysis of gene expression

Abbreviations
5-FU, 5-fluorouracil; dUTPase, dUTP pyrophosphatase; HCC, hepatocellular carcinoma; IHC, immunohistochemistry; qRT-PCR, quantitative reverse transcription-polymerase chain reaction; SAGE, serial analysis of gene expression.

Correspondence
Masao Honda, MD, Department of Gastroenterology, Kanazawa University Graduate School of Medical Science, 13-1 Takara-Machi, Kanazawa, Ishikawa 920-8641, Japan
Tel: +81 76 265 2233
Fax: +81 76 234 4250
e-mail: mhonda@m-kanazawa.jp

Received 13 August 2009
Accepted 26 October 2009

DOI:10.1111/j.1478-3231.2009.02177.x

Abstract

Background: Hepatocellular carcinoma (HCC) is a malignancy with a poor prognosis, partly owing to the lack of biomarkers that support its classification in line with its malignant nature. To discover a novel molecular marker that is related to the efficacy of treatment for HCC and its biological nature, we performed serial analysis of gene expression (SAGE) in HCC, normal liver and cirrhotic liver tissues. *Methods:* Gene expression profiles of HCC tissues and non-cancerous liver tissues were obtained by SAGE. Suppression of the target gene by RNA interference was used to evaluate its role in HCC *in vitro*. The relation of the identified marker and prognosis was statistically examined in surgically resected HCC patients. *Results:* We identified significant over-expression of *DUT*, which encodes dUTP pyrophosphatase (dUTPase), in HCC tissue, and this was confirmed in about two-thirds of the HCC samples by reverse-transcription polymerase chain reaction ($n = 20$). Suppression of dUTPase expression using short interfering RNAs inhibited cell proliferation and sensitized HuH7 cells to 5-fluorouracil treatment. Nuclear dUTPase expression was observed in 36.6% of surgically resected HCC samples ($n = 82$) evaluated by immunohistochemistry, and its expression was significantly correlated with the histological grades ($P = 0.0099$). Notably, nuclear dUTPase expression correlated with a poor prognosis with statistical significance (HR, 2.47; 95% CI, 1.08–5.66; $P = 0.032$). *Conclusion:* Taken together, these results suggest that nuclear dUTPase may be a good biomarker for predicting prognosis in HCC patients after surgical resection. Development of novel dUTPase inhibitors may facilitate the eradication of HCC.

Hepatocellular carcinoma (HCC) is the fifth most common malignancy and the third leading cause of cancer-related death worldwide (1). Several risk factors are responsible for HCC development, including alcoholism, aflatoxin and genetic diseases such as haemochromatosis and α-1 antitrypsin deficiency; however, the major risk factor is chronic hepatitis owing to hepatitis B virus (HBV) or hepatitis C virus (HCV) infection (2–4). Several treatment options are currently available for HCC management, which include liver transplantation, surgical resection, percutaneous ethanol injection, radio-frequency ablation, transcatheter arterial chemoembolization and systemic or local chemotherapy, and optimal treatment is determined based on tumour stage and liver function (5, 6). However, more than 80% of HCC cases develop advanced HCC after initial treatment (7).

Various chemotherapeutic drugs have been investigated for their antitumour activity in advanced HCC. For example, 5-fluorouracil (5-FU), a thymidylate synthase inhibitor, was the first reported drug studied for the treatment of advanced HCC; however, a median survival rate of 3–5 months has discouraged the further use of 5-FU as a single chemotherapeutic agent (8, 9). Interferon-α (IFN-α) has been reported to have antitumour activity against advanced HCC, and recent reports have suggested the efficacy of a combination of 5-FU/IFN-α for advanced HCC treatment (10–12), although convincing evidence for improved survival rate remains lacking. A recent study has indicated that 16% of advanced HCC patients responded positively to 5-FU/IFN-α treatment with clear and significant survival benefits compared with stable or progressive disease

patients (13). Thus, drug sensitivity appears to be one of the major determinants of the prognosis of advanced HCC patients treated with chemotherapy. Therefore, a hallmark of successful treatment would be the identification of useful biomarkers for determining the survival benefits offered by each treatment strategy.

In this study, we investigated the gene expression profiles of HCCs using serial analysis of gene expression (SAGE) to identify novel molecular markers or targets for the treatment of HCC (14–18). Here, we identified the upregulation of the *DUT* gene that encodes dUTP pyrophosphatase (dUTPase) in HCC. Markedly, HCC with a high nuclear dUTPase expression correlated with a poorly differentiated morphology and a poor prognosis. *DUT* gene knockdown not only suppressed cell proliferation but also sensitized HuH7 cells to low-dose 5-FU.

Materials and methods

Samples

All HCC tissues, adjacent non-cancerous liver tissues and normal liver tissues were obtained from 110 patients undergoing a hepatectomy between 1997 and 2006 in Kanazawa University Hospital, Kanazawa, Japan. Five normal liver tissue samples were obtained from patients undergoing surgical resection of the liver for the treatment of metastatic colon cancer. These samples were snap-frozen in liquid nitrogen immediately after resection. One hundred and five HCC and surrounding non-cancerous liver samples were obtained from patients undergoing surgical resection of the liver for HCC treatment, and part of these samples were used for the recent study (19). Three HCC and adjacent non-cancerous liver tissue samples were snap-frozen in liquid nitrogen and later used for SAGE. Twenty HCC tissues and their corresponding non-cancerous liver tissues were also snap-frozen and later used for real-time reverse transcription-polymerase chain reaction (RT-PCR) analysis, as described previously (19). Eighty-two additional HCC samples were formalin-fixed, paraffin-embedded and used for immunohistochemistry (IHC). HCC and adjacent non-cancerous liver tissues were histologically characterized, as reported elsewhere (19).

All strategies used for gene expression analysis as well as tissue acquisition processes were approved by the Ethics Committee and the Institutional Review Board of Kanazawa University Hospital. All procedures and risks were explained verbally to each patient, who then provided written informed consent.

Serial analysis of gene expression

Total RNA was purified from each homogenized tissue sample using a ToTally RNA extraction kit (Ambion Inc., Austin, TX, USA), and polyadenylated RNA was isolated using a MicroPoly (A) Pure kit (Ambion). A total of 2.5 μg of mRNA per sample was analysed by SAGE (20, 21). SAGE libraries were randomly sequenced at the Genomic Research Center (Shimadzu-Biotechnology, Kyoto, Japan), and the sequence files were analysed with SAGE 2000 software. The size of each SAGE library was normalized to 300 000 transcripts per library, and the abundance of transcripts was compared with SAGE 2000 software. Monte Carlo simulation was used for selecting genes whose expression levels were significantly different between the two libraries (22). Each SAGE tag was annotated using a gene-mapping website SAGE Genie database (http://cgap.nci.nih.gov/SAGE/) and the Source database (http://smd.stanford.edu/cgi-bin/source/sourceSearch), as described previously (23).

Quantitative reverse transcription-polymerase chain reaction

A 1 μg aliquot of each total RNA was reverse-transcribed using SuperScript II reverse-transcriptase (Invitrogen, Carlsbad, CA, USA). Real-time RT-PCR analysis was performed using the ABI PRISM 7700 sequence detection system (Applied Biosystems, Foster City, CA, USA). Using the standard curve method, quantitative PCR was performed in duplicate for each sample–primer set. Each sample was normalized relative to β actin. The assay IDs used were Hs00798995_s1 for dUTPase and Hs99999903_m1 for β actin.

RNA interference targeting *DUT*

Small interfering RNAs (siRNAs) targeting *DUT* or control (scrambled sequence) were synthesized by Dharmacon (Dharmacon Research Inc., Lafayette, CO, USA). The target sequences of *DUT* are 5′-AAGUUGU GAAAACGGACAUUC-3′ (DUT1) and 5′-CGGACAUU CAGAUAGCGCUTT-3′ (DUT2). Lipofectamine 2000™ reagent (Invitrogen) was used for transfection according to the manufacturer's instructions.

Cell proliferation assay, soft agar assay and matrigel invasion assay

Cell proliferation assays were performed using a Cell Titer96 Aqueous kit in quintuplicate (Promega, Madison, WI, USA). For the soft agar assay, 1×10^4 cells were suspended in 2 ml of 0.36% agar with growth medium and added in each well of a six-well plate containing a base layer of 0.72% agar. The plates were incubated at 37 °C in a 5% CO_2 incubator for 2 weeks. Matrigel invasion assays were performed using BD BioCoat™ Matrigel Matrix Cell Culture Inserts and Control Inserts (BD Biosciences, San Jose, CA, USA), as described in the manufacturer's instruction. 5-FU was obtained from Kyowa Kirin (Kyowa Kirin, Tokyo, Japan). All experiments were repeated at least twice.

Immunohistochemistry

Mouse monoclonal anti-dUTPase antibody M01 (Abnova Corporation, Taipei, Taiwan) and mouse antiproliferating

cell nuclear antigen (PCNA) monoclonal antibody PC10 (Calbiochem, San Diego, CA, USA) were used to evaluate the immunoreactivity of HCC and adjacent non-cancerous liver samples using a Dako EnVision+™ kit (Dako, Carpinteria, CA, USA), according to the manufacturer's instruction. Immunoreactivity was evaluated by determining the percentage of cells expressing dUTPase in the examined fields, graded as low (0–50%) or high (> 50%). The PCNA index was evaluated as described previously (19).

Statistical analysis

Student's *t*-test was used to determine the statistical significance of the differences in cell viability between the two groups. The Mann–Whitney *U*-test was used for the analysis of gene expression between chronic liver disease (CLD) and HCC tissues. The χ^2-test was used to evaluate the correlation between clinicopathological characteristics and dUTPase expression status. Univariate and multivariate Cox proportional hazards regression analysis was used to evaluate the association of dUTPase expression and clinicopathological parameters with patient outcome. All statistical analyses were performed using SPSS software (SPSS software package; SPSS Inc., Chicago, IL, USA) and GRAPHPAD PRISM software (GraphPad Software Inc., La Jolla, CA, USA).

Results

Gene expression profiling identified the overexpression of *DUT* in hepatocellular carcinoma

To overcome the considerable individual variability of transcriptomic characteristics, we constructed a SAGE library of normal human liver using RNAs derived from five normal liver tissues. In addition, we constructed two SAGE libraries derived from three HCC tissues or corresponding non-cancerous liver tissues from patients who developed HCC with a history of chronic hepatitis C. We detected a total of 226 267 tags corresponding to 45 746 unique tags from these SAGE libraries (supporting information Table S1). After excluding the tags detected only once in each library, we selected 15 333 reliable unique transcripts expressed in at least one of the SAGE libraries to avoid contamination of tags derived from sequence errors. Then, we annotated these transcripts using SAGE Genie database and the Source database to identify the potential subcellular localization of transcripts categorized into eight groups in each SAGE library.

The number of nuclear component-related transcripts was increased in the HCC library compared with the normal liver and non-cancerous liver libraries, whereas the other cellular component-related transcripts did not show this tendency (supporting information Fig. S1). Because nuclear component-related genes may closely correlate with cancer cell proliferation and chemosensitivity (24), we further investigated the expression of nuclear component-related tags in each library, and identified 10 transcripts associated with nucleotide/nucleoside metabolism that are overexpressed in HCC (Table 1). Using Monte Carlo simulation, we evaluated the significance of differentially expressed transcripts in HCC and corresponding CLD libraries or in HCC and normal liver libraries. We identified a *DUT* gene encoding dUTPase (dUTPase) whose expression was significantly altered ($P = 0.01$). We also identified a *TS* gene encoding thymidylate synthase in the list, but the difference did not reach statistical significance.

dUTPase is a phosphatase known to maintain a dUMP pool by catalysing the hydrolysis of dUTP to dUMP, and thus provides a substrate of thymidylate synthase. Its role in HCC is unknown; therefore, we examined *DUT* expression in 20 independent HCC and corresponding non-cancerous liver tissues, and identified significant overexpression of *DUT* in HCC tissue ($P = 0.0015$) (Fig. 1A). Moreover, we detected more than a two-fold increase in *DUT* expression in 70% of HBV-related and HCV-related HCC cases (14 of 20 HCCs) compared with the non-cancerous liver tissues (Fig. 1B). We further examined the expression of *DUT* in 238 HCC tissues compared with the non-cancerous liver tissues using publicly available microarray data (GSE5975) (Fig. S2). Consistent with the SAGE data, *DUT* was overexpressed more than two-fold in 121 of 238 HCC tissues (median: 2.03), whereas *TS* was overexpressed more than two-fold in 54 of 238 HCC tissues (median: 1.41) compared with the non-cancerous liver tissues.

Pivotal role of dUTP pyrophosphatase expression in cell proliferation in hepatocellular carcinoma cell lines

In general, cancer gene signatures discovered by comparison between tumour and non-tumour tissues are more likely to reflect the differences in the control of cell proliferation and growth (25). Accordingly, we investigated the function of dUTPase in cell proliferation in HuH7 cells by *DUT* gene knockdown. *DUT* expression was decreased by 60–70% following the transfection of the siRNA constructs specifically targeting *DUT* 48 h after transfection (DUT1 in Fig. 2A and DUT2 in Fig. S3A), and cell growth was significantly inhibited compared with the control 72 h after transfection (Fig. 2B and Fig. S3B). Anchorage-independent cell growth was also significantly impaired by *DUT* gene knockdown 14 days after transfection (Fig. 2C). Furthermore, *DUT* gene knockdown decreased the numbers of both migrating and invading cells 72 h after transfection (Fig. 2D and E).

dUTPase is known to be associated with thymidylate synthesis (26), and thus we evaluated the effects of 5-FU, a thymidylate synthase inhibitor, on dUTPase expression in HCC cell lines *in vitro*. When we treated HuH7 cells with low-dose 5-FU (0.25 mg/ml), we could not detect any growth-inhibitory effects (Fig. 2F). Based on this condition, we evaluated the effect of *DUT* gene knockdown on 5-FU sensitivity 72 h after transfection.

Table 1. Genes associated with nucleic acid metabolism overexpressed in hepatocellular carcinoma

Tag sequence	Normal liver	Non-cancerous liver	HCC	Fold*	Gene	*P*-value†
CAGCTCCGCT	0	2	11	5.5	dUTP pyrophosphatase	0.010
AAAGGATAAT	0	0	3	> 3	General transcription factor II H, polypeptide 2	0.127
ACGGTCCAGG	0	0	3	> 3	Cytidine deaminase	0.127
ATGTAGAGTG	0	0	3	> 3	Thymidylate synthase	0.127
TGGGGATTAC	1	0	3	> 3	Zinc ribbon domain containing, 1	0.127
CACCCTGTAC	2	2	6	3	Solute carrier family 29	0.147
GAACGCCTAA	1	1	3	3	Dihydropyrimidinase-like 2	0.308
GCGCTGGTAC	0	1	3	3	2′-5′-oligoadenylate synthetase 3	0.308
CTTAGTGCAA	0	2	4	2	3′-phosphoadenosine 5′-phosphosulphate synthase 2	0.335
TTGTTACATC	0	2	3	1.5	Phosphoribosyl pyrophosphatase synthetase-associated protein 1	0.506

*Fold increase was calculated by dividing the number of tags in HCC by that of tags in non-cancerous liver. To avoid division by 0, a tag value of 1 was used for any tag that was not detectable in one sample.

†Statistical significance of differentially expressed genes between two groups (HCC and non-cancerous liver libraries) was calculated using Monte Carlo simulation.

HCC, hepatocellular carcinoma.

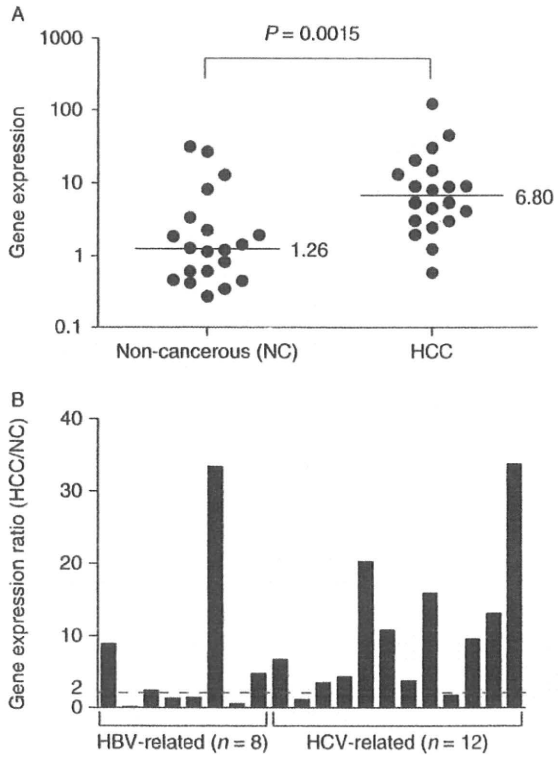

Fig. 1. (A) Quantitative reverse transcription-polymerase chain reaction analysis of *DUT* expression in hepatocellular carcinoma (HCC) and corresponding non-cancerous liver tissues. *DUT* was significantly activated in HCC tissues compared with non-cancerous liver tissues ($P = 0.0015$). A median value in each group is indicated. (B) *DUT* gene expression ratios of HCC and corresponding non-cancerous liver tissues. Fourteen of 20 HCC tissues expressed *DUT* more than two-fold compared with the background non-cancerous liver tissues. HBV, hepatitis B virus; HCV, hepatitis C virus.

Interestingly, *DUT* gene knockdown not only suppressed cell proliferation but also sensitized HuH7 cells to low-dose 5-FU (Fig. 2F and Fig. S3B). These data suggest that dUTPase overexpression in HCC tissues may be associated with enhanced cell proliferation and 5-FU resistance.

Intense dUTP pyrophosphatase expression is correlated with a poor prognosis in hepatocellular carcinoma patients

To characterize the clinicopathological characteristics of dUTPase expression in HCC, we performed IHC using an additional independent HCC cohort. Accordingly, we explored the dUTPase expression in HCC using 82 formalin-fixed paraffin-embedded HCC specimens. All HCC tissues were surgically resected at the Liver Disease Center of Kanazawa University Hospital with full clinical information, and their immunoreactivity to anti-dUTPase antibodies was evaluated by IHC. We noticed that anti-dUTPase antibodies reacted to both nuclear (red arrows) and cytoplasmic (blue arrows) isoforms of dUTPase, as described previously (26) (Fig. 3A and B). We therefore evaluated the nuclear and cytoplasmic expression of dUTPase separately. We stratified HCC tissues and evaluated the dUTPase expression status based on the percentages of dUTPase-positive cells. The frequency of nuclear or cytoplasmic dUTPase-positive cells was highly variable in each HCC tissue, and we defined HCCs with nuclear or cytoplasmic dUTPase expressed in $\geq 50\%$ of tumour cells as nuclear or cytoplasmic dUTPase-high HCC (Fig. 3C). Nuclear dUTPase overexpression was detected in 36.6% (30 of 82), whereas cytoplasmic dUTPase overexpression was detected in 67.1% (55 of 82) of HCC tissues compared with the corresponding non-cancerous liver tissues

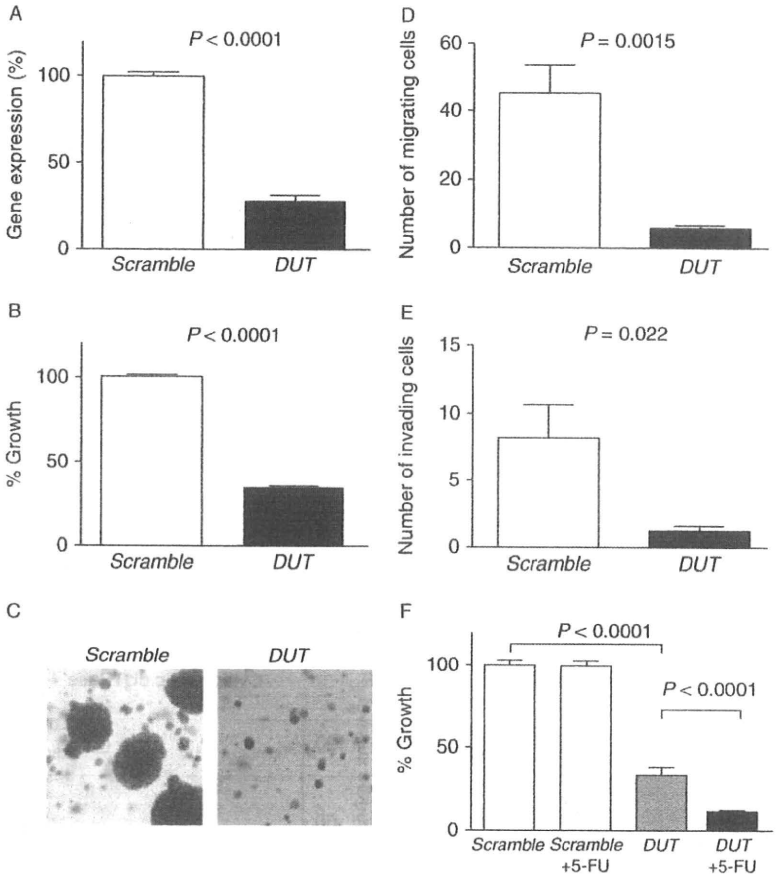

Fig. 2. (A) Transfection of small interfering RNAs targeting *DUT* (DUT1) decreased *DUT* expression compared with the control (scrambled sequence). Gene expression was evaluated in triplicate 72 h after transfection (mean ± SD). (B) *DUT* gene knockdown significantly suppressed cell proliferation ($P < 0.0001$). Cell viability was evaluated in triplicate 72 h after transfection (mean ± SD). (C) Soft agar assay. *DUT* gene knockdown suppressed anchorage-independent cell growth. (D and E) Matrigel invasion assay. *DUT* gene knockdown decreased the numbers of both migrating and invading cells. Experiments were performed in triplicate (mean ± SD). (F) *DUT* gene knockdown sensitized HuH7 cells to low-dose 5-fluorouracil (5-FU) (0.25 μg/ml), which had no effect on the cell proliferation in the control (mean ± SD).

(Table 2). In general, non-cancerous hepatocytes rarely expressed nuclear dUTPase (Fig. 3A).

We investigated the clinicopathological characteristics of nuclear or cytoplasmic dUTPase in low /high HCC cases (Table 2). The expression status of nuclear dUTPase showed no correlation with age, gender, virus, presence of cirrhosis, α-fetoprotein value, tumour size and TNM stages. However, nuclear dUTPase expression was significantly correlated with the histological grades of HCC ($P = 0.0099$), and high frequencies of nuclear dUTPase-positive cells were associated with poorly differentiated cell morphology in the HCC tissue. In contrast, cytoplasmic dUTPase expression was not correlated with the histological grades of HCC ($P = 0.077$). We examined the cell proliferation of these HCC samples by PCNA staining, and PCNA indexes were significantly higher in nuclear dUTPase high HCC than low HCC with statistical significance ($P = 0.01$) (Fig. S4).

We further investigated the prognostic significance of dUTPase expression in HCC. Strikingly, high nuclear dUTPase expression in HCC tissue correlated with a poor survival outcome compared with low nuclear dUTPase expression ($P = 0.0036$), whereas high cytoplasmic dUTPase expression had little effects when evaluated by recurrence-free survival (Fig. 3D). Furthermore, univariate Cox regression analysis showed a significant correlation between high nuclear dUTPase expression and a high risk of mortality (HR, 2.47; 95% CI, 1.08–5.66; $P = 0.032$; Table 3). By multivariate Cox regression analysis, TNM stage (HR, 2.75; 95% CI, 1.11–6.79; $P = 0.027$) and nuclear dUTPase (HR, 2.61; 95% CI, 1.13–6.05; $P = 0.024$) were independent prognostic factors associated with a high risk of mortality, and other clinicopathological features did not add independent prognostic information. These data indicate a significant correlation between the malignant potential of